WAVE PROPAGATION AND DAMAGE CHARACTERIZATION IN NATURAL FIBER HEMP AND LLDPE COMPOSITE

A Thesis

by

SANDIP HODKHASA

Submitted to the Office of Graduate Studies of
Texas A&M University
in partial fulfillment of the requirements for the degree of

MASTER OF SCIENCE

Approved by:

Chair of Committee,	C. Steve Suh
Committee Members,	Terry Creasy
	Ramesh Talreja
Head of Department,	Jerry Caton

May 2013

Major Subject: Mechanical Engineering

ABSTRACT

Research in incorporating natural fibers in composites has been in progress for a few decades where the various mechanical, electrical and acoustic properties of such composites were explored. Natural fiber composites (NFCs) have few benefits over the traditional glass or carbon fiber composites such as light weight, low manufacturing cost and requiring less energy for production. NFC is also bio-degradable and recyclable. The primary objectives of this research are to explore the static and dynamic properties of the hemp and linear low density polyethylene (LLDPE) and determine impact absorbing capability using the above mentioned properties.

LLDPE is surface-treated with maleic anhydride grafted polyethylene (MA-g-PE) and sodium hydroxide (NaOH). A melt-mixing process is employed where LLDPE is compounded with the hemp fibers in 10%, 20% and 30% vol. fraction. Tensile and flexural properties are measured. The material is characterized by propagating Lamb waves generated using a dropped dead weight. Time-frequency information is extracted from a thin disc-like specimen using the Gabor Wavelet Transform (GWT) so as to characterize the material. Detection of defect is also established using the generated waves and GWT. Using Gabor wavelet coefficients, the dispersion and attenuation of the specimen are determined in different material directions. Comparison of attenuation of the waveforms is observed at different locations providing the knowledge of materials homogeneity, the materials behavior due to an impact and its impact absorbing character.

ACKNOWLEDGEMENTS

I would like to give my sincere acknowledgment to Dr. Steve Suh for being a phenomenal mentor throughout these years of my study at Texas A&M University. His insight to my research has been profound. His motivational words have helped me through my struggling days.

I would like to convey my regards to Dr. Creasy for his acute input and generosity towards my research. I also would like to mention his student, Gene Cha, for his help. I would like to commend Dr. Talreja for his advice on my study.

My lab-mates Jason Meng-Kun Liu , Chi-Wei Kuo and Eric Halfmann have also given valuable input to my research. I would like to mention Dr. H. J. Sue and his student Peng Liu, too. My thanks also go to the departmental faculty and staff for making my time at Texas A&M University a great experience.

Many friends of mine have supported me throughout these years. Shawn Oosman, Anish Dharia, Dana Sahadeo, Pallavi Rambhasha, Bhargav Kottapalli, Ashanth Narain, Jai Lopez and several others along with my brothers and sisters have helped in every possible way. I am grateful for their support.

My greatest expression of gratitude goes to my parents for their unconditional love and support in my endeavor.

NOMENCLATURE

LLDPE	Linear Low Density Polyethylene
NFC	Natural Fiber composite
OH	Hydroxyl
NaOH	Sodium Hydroxide
MA-g-PE	Maleic Anhydride Grafted Polyethylene
MPa	Mega Pascal
GPa	Giga Pascal
HDPE	High Density Polyethylene
DDA	Steam Explosion Process
BIA	Biological Separated Fibers
PEA	Co-polyesteramide
PLA	Polylactic Acid
PP	Polypropylene
FT	Fourier Transform
GWT	Gabor Wavelet Transformation
Loc	Location
UNHEMP	Untreated Hemp Fibers
NAHEMP	Sodium Hydroxide Treated Hemp Fiber
MAGHEMP	Maleic Anhydride Grafted Polyethylene Treated Hemp Fiber
MFI	Melt Flow Index

CFRP	Carbon Fiber Reinforced Polymer
GFRP	Glass Fiber Reinforced Polymer
PZT	Piezoelectric Transducers
SD	Standard Deviation
CV	Coefficient of Variance
HEMP-LLDPE	Hemp and LLDPE Composite

TABLE OF CONTENTS

Page

LIST OF FIGURES

Page

LIST OF TABLES

1. INTRODUCTION

1.1 Objective

The purpose of the research is to study a new natural fiber composite of hemp and linear low density polyethylene (LLDPE) and explore the dynamic properties of the material such as attenuation factor and dispersion. This research aims to explore the material's homogeneity and quantify if uniform homogeneity has been achieved due to the manufacturing process of the composite. At the same time, post damage attenuation and dispersion property of the composite are investigated. Comparing the post-damage results with pre-damage results would establish if the material's behavior changes drastically with the defects. The research also proposes the use of the hemp and LLDPE composite in various industrial applications, as well as discusses the replacement of traditional materials with NFCs on the basis of the latter being cheaper and lighter while providing similar properties compared to the former ones. Hence the NFC would be manifested as cost-efficient, lighter and recyclable giving an edge over other materials and commonly employed in industries such as

- Automobile industry: to replace car bumpers and interior panels to absorbs impact from collision.
- Consumer industry: to replace parts made of toxic, non-degradable plastics.
- Emergency relief aid: to build temporary huts and mobile camps to aid relief victims.

Materials having high dispersion and attenuation factors in general perform better in resisting impact and in dissipating the shock waves induced by the impact.

Non-destructive testing (NDT) comes very handy in determining material characteristics and damage identification. Lamb waves generated due to an impact (by dropping a dead weight) in thin samples are processed using GWT. GWT provides results that depict the characteristics of the material along primary axis and determine the homogeneity of the material, hence also help in speculating the need to alter various processing factors that could aid in achieving consistent property of the material.

Using GWT, the dynamic properties of the material are determined such as dispersion and attenuation factor. If the material is found to be highly dispersive with high attenuation factor, then the material has an energy dissipation property and it could be considered to have high impact resistance property.

This research also explores the after-damage property of the material. Artificial damage is inflicted, wave dispersion and attenuation factor are then determined post damage infliction and the change in the dynamic properties is established in order to speculate if artificial holes and damages would help the impact property of the material.

1.2. Natural Fiber Composites (NFCs)

Composite materials are a combination of two or more materials that are artificially combined through various processes. The materials are combined using different procedures to obtain different composites properties. There are different variables involved in the process of fabricating composites. The change of these variables can change the material's characteristics and properties. A typical composite is made of minimum two materials such as a polymeric matrix and fibers. The polymer could be thermoplastics such as Polypropylene, while conventionally, the fibers used are

glass fibers or carbon fibers. The fibers can be continuous or discontinuous depending on the property desired.

With their many preferred properties, composites have been used in a wide range of applications in aerospace, electronics, and bio-medical industries, to name just a few. A composite has wide range of properties, some of the properties are listed below [1]:

- Low density compared to various metals
- High strength and stiffness
- Good impact resistance and toughness
- High damping capacity
- Corrosion resistance

Apart from employing carbon and glass fibers as the reinforcing materials and polymers as matrix material, there are other materials that are extensively used to create a composite which are applied in various industries, such as cement, metal, ceramics as a matrix materials whereas natural fibers and nano-fillers are some of the reinforcements used in composites. With different types of composites available, there are also different types of problems associated with these composites. Few of the primary issues are disposing of the toxic ingredients and the ability to recycle; these were few of the reason that compelled the researchers to look into bio-degradable polymers and natural fibers.

Natural fibers in composites have been in implementation for many centuries. In the era of Egyptians (1500BC) bamboo shoots with laminated wood were used for housing purposes. Natural fibers were also used with metals for making swords (1800AD) [2]. During the early 19^{th} century, the usage of carbon fiber and glass fiber

composites came into play. Late 1970s saw an increase in research of natural fiber composites, primarily due to the following reasons: low manufacturing cost and advantage of having the properties of recyclability and bio-degradability. The density of glass fiber is found to be 2.6gm/cc with a cost of $1.30 to $2.00/kg when compared with natural fibers having a density of less than 1.5gm/cc and priced at $0.22 and $1.10/kg [3]. Joshi and others [3] mentioned about the environmental effect of the production of Hemp-epoxy composite which is almost half compared to ABS copolymers when they were used to produce automotive panels. It was shown in [3] that the energy required for the production of fiberglass mats was 54.7 MJ/kg as compared to flax fiber mats which required only 9.55 MJ/kg.

Natural fibers are generally categorized as seed, leaf and bast fibers. Some of the examples of the fibers are cotton (seed fibers), ramie, jute and flax (bast fibers), and sisal (leaf fibers). The chemical components of the natural fiber in general consist of cellulose, hemicellulose, lignin, pectin, waxes and other water soluble substances but the composition of these chemical components are highly depend on the growing condition and weather. Cellulose is a semi-crystalline polysaccharide. The high content of hydroxyl ions in cellulose is responsible for the hydrophilic nature of the natural fiber. Hemicelluloses binds with cellulose fibrils presumably by hydrogen bonds while lignins are highly complex structures and are least soluble in water [4].

2. LITERATURE REVIEW

2.1. Natural Fiber and Its constituents

There has been an exclusive research taking place in the field of natural fiber composites, which roughly commenced around 1970's. The typical properties of natural fibers that have intrigued researchers are low density, low cost for production, low energy absorption, biodegradability, and recyclability.

Natural fibers are extracted from animal source and plants. Natural fibers that are derived from plants are frequently used in industrial applications. Some of the examples of these fibers are hemp, jute, flax, cotton sisal ramie and others. The Plant fibers can be divided into the following categories [5]:

- Bast fibers - They are extracted from the inner bark of the plants. The bark provides the strength and structural support to the plant. Some of the bast fibers are jute, flax, hemp and ramie.
- Leaf fibers – These types of fibers are also known as hard fibers. They are obtained from leaves and flowering plants having parallel veins. Example of such long and stiff fibers are banana, henequen, sisal and others [6].
- Seed fibers – They are typical fibers that are known to be grown around the seed or in the seed. Known to be long, soft and fluffy, some of the examples are cotton, coir, and kapok.
- Core fibers – Core fibers are found inside the bast fibers. They are short fibers such as hemp, jute, kenaf and others.
- Grass and other fibers - Bamboo and wood are some of the popular ones.

Natural fibers are chemically composed of several constituents such as cellulose, hemicellulose, lignin, pectin, waxes and other water soluble substances. As mentioned earlier these chemical constitutes affects the mechanical properties of the fiber and the percentage of the chemical constituents in the fibers are completely dependent on the growing conditions. Followings are a brief introduction of the fiber constituents [4]:

- Cellulose – They are a semi-crystalline structures made of high amount of hydroxyl groups. These hydroxyl groups give the fiber a hydrophilic property, i.e. the tendency to absorb moisture.
- Hemicellulose – These are fibrils that are believed to have hydrogen bonds among them. They are amorphous in structure with low molecular weight. Hemicellulose is also known to be soluble in water.
- Lignins – Lignins are known to be amorphous and highly complex in nature. They are naturally resistant to degradation [7].
- Pectin – Pectin is another type of substance that is found in plant cells that are known to associate with lignin and hemicelluloses. They are also hydrophilic in nature and known to have structures of long chains [8].

Once the basic elements of the fibers are known, chemical modification can be performed accordingly to remove the unnecessary structure and optimize the adhesion between the fiber and polymeric matrix. Table 1 [4] provides a general list of property and composition of some natural fibers

Table 1 Properties and chemical composition of natural fibers

Fiber	Density g/cc	Young's Modulus (GPA)	Tensile Strength (MPA)	Cellulose (%)	Hemicellulose (%)	Lignin (%)
Cotton	1.5-1.6	5.5-12.6	287-597			
Jute	1.3-1.4	10-30	393-800	45-71	13.6-21	12-26
Flax	1.4-1.5	27.6-80	345-1500	43-47	24-26	21-23
Hemp	1.26-1.48	70	550-900	57-77	14-22.4	3.7-13
Sisal	1.3-1.5	9-38	400-700	47-78	10-24	7-11
Ramie	1.5	44-128	220-938	68-91	0.6-0.7	5-16.7
Glass Fiber	2.5	70	2000-3500			
Carbon Fib.	1.8	240	4500			

2.2. Surface Treatment

Due to the moisture absorbing property of natural fibers, the fibers show poor bonding with the polymer matrix (polymers are known to be hydrophobic in nature, i.e. resisting the absorption of water.) Hence there is a need to use chemical agents or compatibilizers that help increase the interfacial adhesion between the fibers and the base polymers. Since cellulose and hemicellulose (the chemical constituents of the fibers) contains the maximum amount of hydroxyl group ions, therefore, the idea is to improve the compatibility of the fibers by eliminating these hydroxyl ions. The compatibility between the fibers and the polymers is also increased by modifying the matrix properties [5]. Listed below are some of the widely used chemical treatments.

2.2.1. Alkaline Treatment

Alkaline treatment also known as mercerization is one of the most used chemicals to perform a surface treatment [4] on the fibers when reinforced into polymers. The treatment is done by soaking the fibers in the aqueous solution of Sodium hydroxide (NaOH). The treatment uses the following reaction

$$(\boldsymbol{Fiber - OH}) + \boldsymbol{NaOH} \rightarrow (\boldsymbol{FIber - O - Na}) + \boldsymbol{H_2O} \quad (1)$$

The treatment removes the hydroxyl group, wax, oil, and other substances that cover the cell wall of the fiber. This process directly involves the cellulose, hemicellulose and lignin. Ray et al. [9] have treated jute fibers with 5% aqueous solution for 2 hours, while Morrison et al [10] have treated flax fibers in an alkaline solution of 2% for 90s. It was observed that the solution increased the amorphous cellulose content [4]. Rong et al [11] had submerged sisal fibers in a 2% NaOH solution for 4 hours.

2.2.2. Silane Treatment

Silane treatment is the next most popular treatment after alkaline treatment. The compound used in this process is mainly organo-silanes. The organo-functional group of the silanes reacts with the fiber to increase the adhesion. Silanes react with water to form silanols that react with the cellulose hydroxyl group of the fiber. They form a stable covalent bond with the cell wall [12]. The following reaction takes place in the treatment:

$$\boldsymbol{CH_2CHSi(OC_2H_5)_3} \xrightarrow{\boldsymbol{H_2O}} \boldsymbol{CH_2CHSi(OH)_3 - 3C_2H_5OH} \quad (2)$$

$$\boldsymbol{CH_2CHSi(OH)_3 + (Fiber - OH) \rightarrow CH_2CHSi(OH)_2O - Fiber + H_2O} \quad (3)$$

Rong et al. [11] treated sisal fibers with 2% aminosilane in 95% alcohol. They carried out the treatment for 300s so as to have a pH value of 4.5–5.5. Later the fibers were dried in air. Sawpan et al. [13] used a 0.5 wt% silane coupling agent solution that was prepared in Acetone. They submerged hemp fibers for 45-min in the solution and the fibers were dried in oven at 65^{O}C for 12 h.

2.2.3. Acetylation Treatment

In this process the fibers are soaked into acetic anhydride. Soaking the fibers accelerate the reaction [14]. Therefore, the fibers should be soaked in the chemical for 1-to-3 hours. The process swells the cell wall of the plant fibers and reduces the hydrophilic nature of the fiber. The reaction also involves the acetyl functional group and produces acetic acid as a by-product. The reaction in this type of treatment is shown below

$$\boldsymbol{Fiber - OH + CH_3 - O(=O) - O - C(=O) - CH_3} \rightarrow \boldsymbol{Fiber - OCOCH_3 + CH_3COOH} \quad (4)$$

Rong et al. [11] also treated sisal fibers in a 18% NaOH solution for 5-min. The fiber was then soaked in 50% acetic acid aqueous solution for 5-min and then air dried.

2.2.4. Isocynate Treatment

Isocynate process involves two steps in which the fibers are first washed with the NaOH solution and afterward they are treated with carbon tetrachloride. The fibers are then oven-dried. The isocynate group of the compound is known to be highly vulnerable to react with the hydroxyl group of the plant fiber [14]. The 'R' in the equation below is any alkyl group.

$$\boldsymbol{R-N=C=O+OH-Fiber \rightarrow R-(N-H)-(C=O)-O-Fiber} \quad (5)$$

2.2.5. Maleated Coupling Agent

Maleic anhydride is used to treat fibers in this kind of treatment. The fiber and the matrix both are treated with the chemicals to remove the hydroxyl group. Mohanty et al. [15] used maleic anhydride grafted polypropylene with toluene in their research. They treated jute fibers with 0.3%, 0.5% and 1% concentration of maleic anhydride grafted polypropylene in toluene. They claimed that 0.5% concentration of maleic anhydride grafted polypropylene in toluene produced the best mechanical properties.

2.2.6. Other Treatments

There are various other treatments that have been employed for the surface treatment of fibers, the details can be found in [4, 14]. Few of the examples are

- Benzoylation treatment where Benzoyl chloride is used to treat fibers; and
- Peroxide treatment is an inorganic treatment where peroxide is used for a functional group of the formulae R-OO-R, with 'R' being the functional group.

2.3. Process of Composite Preparation

There are various processes available and are very similar to the preparation of traditional composites. It is also imperative to focus on the processing of the natural fiber composites as there are constrains in the processing of the natural fibers. Natural fibers have a ceiling temperature at which the fibers thermally degrades [2] and not all polymeric matrices could be used with natural fibers. Hence the processing temperature plays an important factor. Two of the different methods are mentioned below.

2.3.1. Melt Mixing

Melt mixing is a process of mixing the materials using radial flow. In this process, heat is applied to melt the thermoplastic polymer to a certain temperature inside a small chamber. The chamber has an opening barrel through which the polymers and the fibers are inserted into the chamber. The chamber consists of two screws attached to a motor. The screws rotate in opposite direction. With the continuous rotation of the screw, the melting polymers are mixed with the fibers. The chamber is composed of several plates that are connected to thermocouple. The thermocouple increases the temperature of the chamber by heating up the plates. The temperature of the chamber is set according to the viscosity of the polymer required but at the same the time keeping the temperature low enough to avoid the thermal degradation of the materials. The rotation helps in providing proper distribution of the fiber in the polymer. It is easier to provide a higher dispersion of the fibers with the polymer, if the polymer is very less viscous which could be achieved by having high temperature. There are different types

of screws available to fabricate these composites. Since this is a closed chamber, there is no outlet for adding a mold. Hence the chamber needs to be opened every time after the proper blending of the fibers is achieved. The chamber of such mixer can only provide a blend of less than ~40 gm of material in one batch. Figure 1 [16] shows the cross-section of the mixing chamber where the two screws are shown rotating in opposite direction. The opening in the top is the barrel through which the materials are inserted into the chamber.

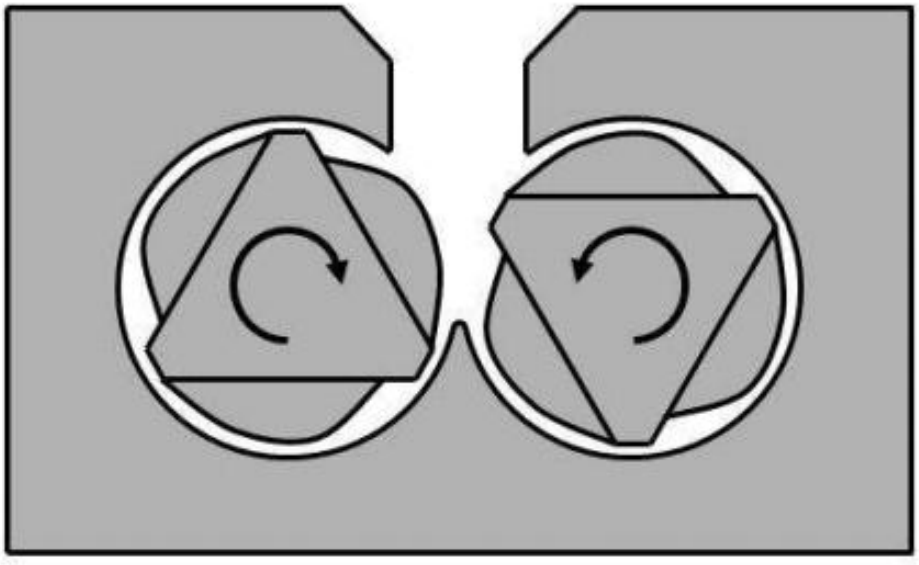

Figure 1. Cross section of the melt-mixing chamber

2.3.2. Compression Molding

Also known as hot pressing, compression molding is widely used for producing composites in large quantity. Compression molding is very handy and easy to use in making products in large scale quantities. Compression molding comes in handy when

the fibers are in the form of woven mats. Thermoplastics are used in a form of sheets and they are placed in a cavity or a mold with fibers. The mold temperature is increased by heating the press, while the press is closed and pressure applied. The pressure applied depends on the type for mold used. Hence for simpler and uncomplicated mold low pressure is applied while for complicated and narrow molds high pressure is applied. The compression molding is made of a hydraulic press with two plates. The plates are heated and are closed using the hydraulic machine. The size of the plates and the pressure depends on the size of the machines from the size of 6in. square to 8ft. square and from 6 to 10,000 tons of pressure. Generally all the compression molding presses are a vertical press where one of the plate is static and the other plate moves up and pushed the mold to close [17]. The Figure 2 (below) shows the schematic of a compression molding machine. The parts labeled are as follows:

A: The Static Plate

B: The Mold on which the pressure is applied

C: The base mold on which the composite mixture is inserted

D: The base plate which is moving

E: The hydraulic section through the pressure is applied.

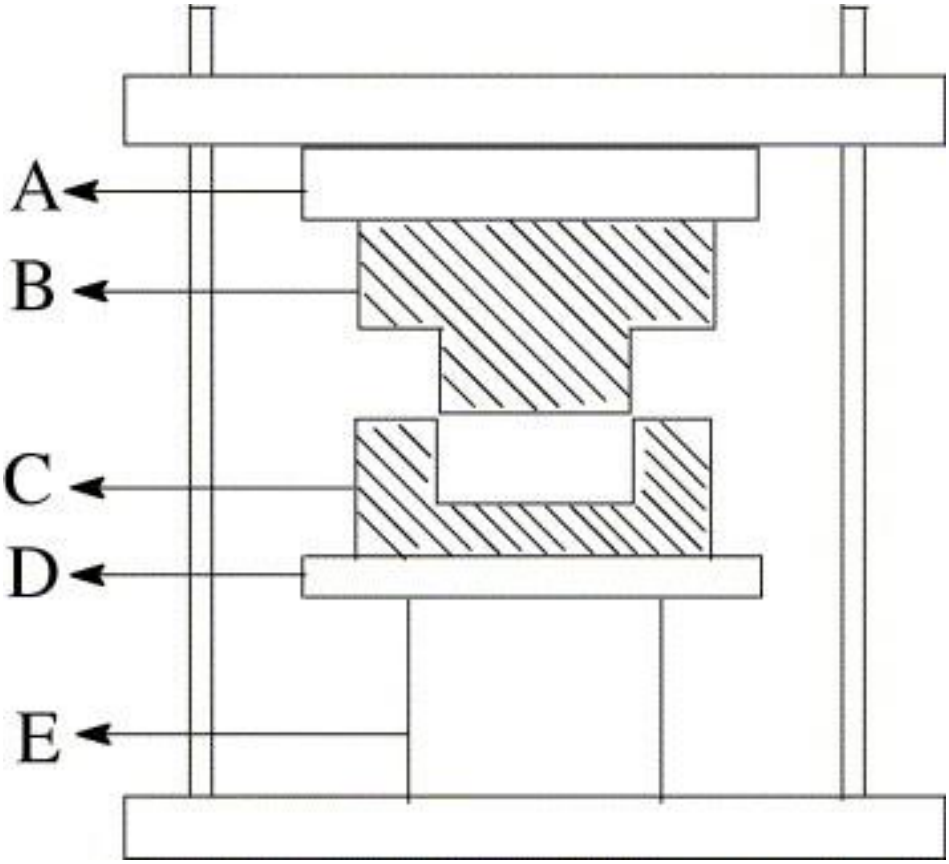

Figure 2. The schematic of a compression molding press

2.4. Hemp and Its Composites

Hemp is also known as *Cannabis Sativa*. It was estimated that China was the largest producer of hemp. Despite the fact, the usage of hemp is just limited to textile industry. Among several other natural fibers hemp is considered to have good mechanical properties [18]. Hemp is a type of bast fibers that are known for having long and stiff fibers. Like most other natural fibers, hemp is mainly composed of cellulose, hemicelluloses, lignin and pectin, and other waxy substances. Table 2 [19] gives the constituents of bast and hurd fibers. Figure 3 [8] shows a cross-section of a stem of *Cannabis Sativa* plant.

Table 2 Constituents of hemp fiber

	Cellulose	Hemicellulose	Pectins	Lignin	Wax + fat	Ash	Proteins
Bast Fiber	55	16	18	4	1	4	2
Hurd Fiber	48	12	6	28	1	2	3

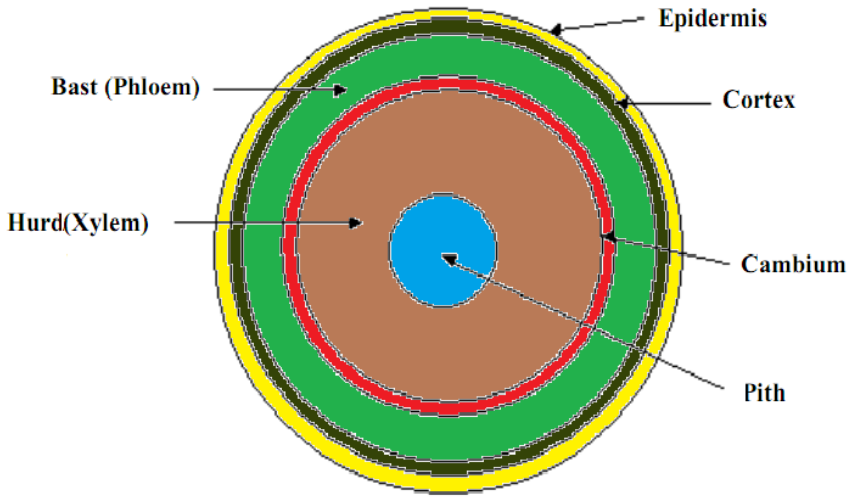

Figure 3. Cross section of *Cannabis Sativa*

Na Lu and et al [20] researched hemp fibers and high-density polyethylene where they treated the fibers with 5% alkali solution and used a single-screw extruder to process the composite. They proved that the usage of NaOH has improved the mechanical properties by two times when compared with the untreated fibers. They also reported the values of 40% vol. of hemp in HDPE for tensile strength, tensile modulus, flexural strength and flexural modulus as 60.2MPa, 2575MPa, 44.6MPa, and 2429MPa, respectively.

Keller [21] used two different types of hemp fibers – a steam explosion process (DDA) and biological separated fibers (BIA). He used biodegradable polymers called co-polyesteramide (PEA) and a poly 3-hydroxybutyrate-co-3hydroxyvalerate (PHBV). Both the fibers and matrix were dried at $60^{O}C$ in vacuum. The processing of the composite was done with injection-molding using a twin-screw extruder. The highest tensile strength was reported to be 29.4 MPa for PEA-DDA at 27% vol. However the highest impact strength for PEA-DDA composite was reported for 10% vol. He also mentioned the cracks were initiated and ran along the interface of the fiber and matrix.

Dhakal et al [22] studied the effect of water absorption on mechanical properties. The polyester matrix was cured using a catalyst known as methyl ethyl ketone peroxide at a conc. of 0.01 w/w of the matrix. Randomly oriented non-woven hemp fibers were used. A combination of a hand lay-up and compression molding was employed to prepare the composite samples. Once the composite were prepared they immersed the specimens for 888 hours. The reported results were a little erratic as the tensile stress measured for moisture-absorbed specimens was higher than moisture-free specimens for 26% vol. of fibers; while 15% and 21% vol. moisture-free specimens recorded higher tensile stress when compared with the same volume fraction of moisture absorbed specimens. The flexural stress of the moisture-absorbed samples reported less values compared to the dry samples.

Hu and Lim [23] fabricated and tested the mechanical properties of hemp and Polylactic acid (PLA). They treated the fibers with NaOH for 24 hours and the fibers were then oven-dried. They placed the PLA film and the short hemp fibers into the mold

layer after layer and then it was compressed with 1.3 MPa. The 40% vol. NaOH treated fibers recorded a tensile strength and flexural strength of 54.6 and 112.7MPa, respectively. Twite and others [24] studied the rheological properties of the polypropylene and hemp treated with maleic anhydride polypropylene. It was found that the use of the chemical had increased the plasticizing effect of the matrix and the interfacial adhesion between the fibers and matrix.

Bledski [25] treated hemp with maleic anhydride polypropylene as a coupling agent and the resins used were polypropylene and epoxy. It was shown that the use of coupling agent in hemp-PP composite increased the flexural strength by 90% when tested unidirectional. The coupling agent also increased the flexural modulus of the composite with epoxy as the resin.

3. WAVES PROPAGATION IN THIN SECTION

3.1. Lamb Waves

Lamb waves were first derived by Horace Lamb in 1917. They generally exist in thin sections with traction-free boundaries. The application of Lamb waves rose during the World War II when they were used for damage detection. Since then Lamb waves have been a prominent tool for Non-destructive evaluation (NDE) and testing [26]. Lamb waves are also known for having high susceptibility to interference on the propagation path. Lamb waves can travel over a long distance even in materials with a high attenuation ratio, such as carbon fiber-reinforced composites, thus allowing a large area to be examined quickly [27]. It is also known that the entire thickness of the plate can also be interrogated to inspect for damage, defect, void, and delamination [27]. Some of the properties of Lamb waves illustratively mentioned in [27] and [28] are:

- the ability to inspect large structures such as a submerged pipe system;
- the ability to inspect large cross-sectional area;
- sensitivity to interference, hence voids are easily be detected.
- generation of the waves is cost-effective

In isotropic materials the equations of motion defined in the Cartesian coordinates are

$$\boldsymbol{\mu \cdot u_{i,jj} + (\lambda + \mu).u_{i,jj} + \rho.f_i = \rho\,.\ddot{u}_i} \qquad \boldsymbol{(i,j = 1,2,3)} \tag{6}$$

where , λ are the Lame's constants and ρ , f are density and body forces, respectively. The above equation can be used to derive the following characteristic equation that defines the various Lamb wave modes that propoagate in thin plate made of isotropic and homogenous material [29]:

$$\frac{\tan(qh)}{\tan(ph)} = \frac{4k^2qp\mu}{(\lambda k^2+\lambda p^2+2\mu p^2)(k^2-q^2)} \tag{7}$$

With h being the plate thickness and

$$p^2 = \frac{\omega^2}{C_L} - k^2;\ \ q^2 = \frac{\omega^2}{C_t} - k^2; k = \omega/c_p$$

3.2. Gabor Wavelet Transformation

An acquired Lamb waveform does not provide comprehensive information about the material property and characteristics. Hence, the waveform needs be transformed into the frequency domain. There are tools available to transform the waveform from the time domain to frequency domain such as the short-time Fourier transform and Wavelet Transformation.

The foundation of these tools is based is the Fourier Transform (FT). FT converts a signal, $x(t)$, which is a function of time to the frequency domain only,

$$X(\omega) = \int_{-\infty}^{\infty} x(t)e^{-i\omega t}dt \tag{8}$$

Though Fourier transform is a convenient tool to use, it has some limitations and does not give a proper depiction of the frequency-dependent waveform. Chirp signal is one example [30]. In order to resolve such an issue, Short Time Fourier Transform was introduced,

$$X(\omega,\tau) = \int_{-\infty}^{\infty} x(t)\psi(t-\tau)e^{-i\omega t}dt \tag{9}$$

here $\psi(t-\tau)$ is a window function. This window function scans the waveform throughout and each scan is represented by a transform function, $X(\omega,\tau)$. Short time

Fourier transform gives a better representation of the waveform travelling in a material, but the resolution is compromised as the resolution is inherently fixed.

The disadvantage of short time Fourier transforms can be overcome with the usage of Wavelet Transformation, which is defined as follows,

$$\boldsymbol{X(a,b) = \frac{1}{\sqrt{a}}\int_{-\infty}^{\infty} x(t)\bar{\psi}(\frac{t-b}{a})dt} \tag{10}$$

where $\bar{\psi}(t)$ is the conjugate function of the mother wavelet, $\psi(t)$. A wavelet is defined as a function with oscillation that is wave-like and compactly supported. A wavelet function must satisfy the following condition

$$\boldsymbol{\int_{-\infty}^{\infty} \frac{|\hat{\psi}(\omega)|}{|\omega|}\, d\omega < \infty} \tag{11}$$

where $\hat{\psi}(\omega)$ is the Fourier transform of $\psi(t)$. The mother wavelet function $\psi(\frac{t-b}{a})$ is centered at 'b'. Therefore changes in 'b' known as the translational parameter will move the window function through the signal. '*a*' is known as the dilation parameter that dictates the scaling of the wave function.

Gabor wavelet function gives the best time and frequency resolutions as

$$\boldsymbol{\psi(t) = \frac{1}{\sqrt{\gamma}}\exp\left(-\frac{t^2}{2\gamma^2}\right)(\cos t + i\, sint)} \tag{12}$$

It can be mathematically proven that based on the uncertainty principle, the Gabor wavelet function offers the smallest time-frequency window, thus giving the best time-frequency resolution [31].

3.2.1. Influence of Gamma - γ in Gabor Wavelet

The Gabor wavelet equation has a certain parameter that controls the shape of the Gabor wavelet function. 'γ' has a great influence on the Gabor wavelet function. The time duration and frequency bandwidth of the Gabor wavelet function are now related with the central frequency: the higher the frequency resolution becomes, the smaller the time duration [32]. The following graphs in Figs. 4 and 5 shows the influence of 'γ' and dilation parameter, '*a*'. In Figure 4 the value of '*a*' is chosen to be 0.1 and the values of γ are 2, 4, 6, and 8. The value of 'b' is centered at zero. Figure 4 shows the increment of the oscillation as γ changes. In Figure 5 the values of the dilation '*a'* is changed to 0.5 while γ is kept the same. It can be seen that, due to the change in dilation '*a'* the waveform has been 'stretched,' while the change in γ induces oscillations in the waveform as previously mentioned.

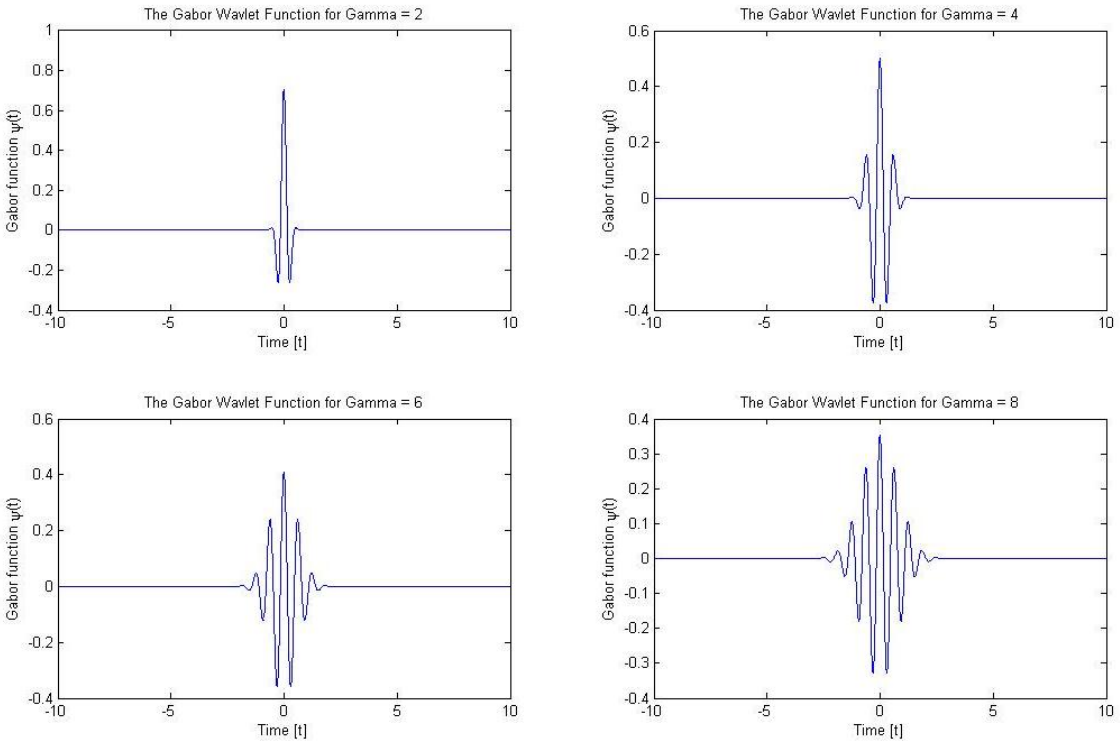

Figure 4. Gabor wavelet function with $a = 0.1$ and $\gamma = 2, 4, 6$, and 8

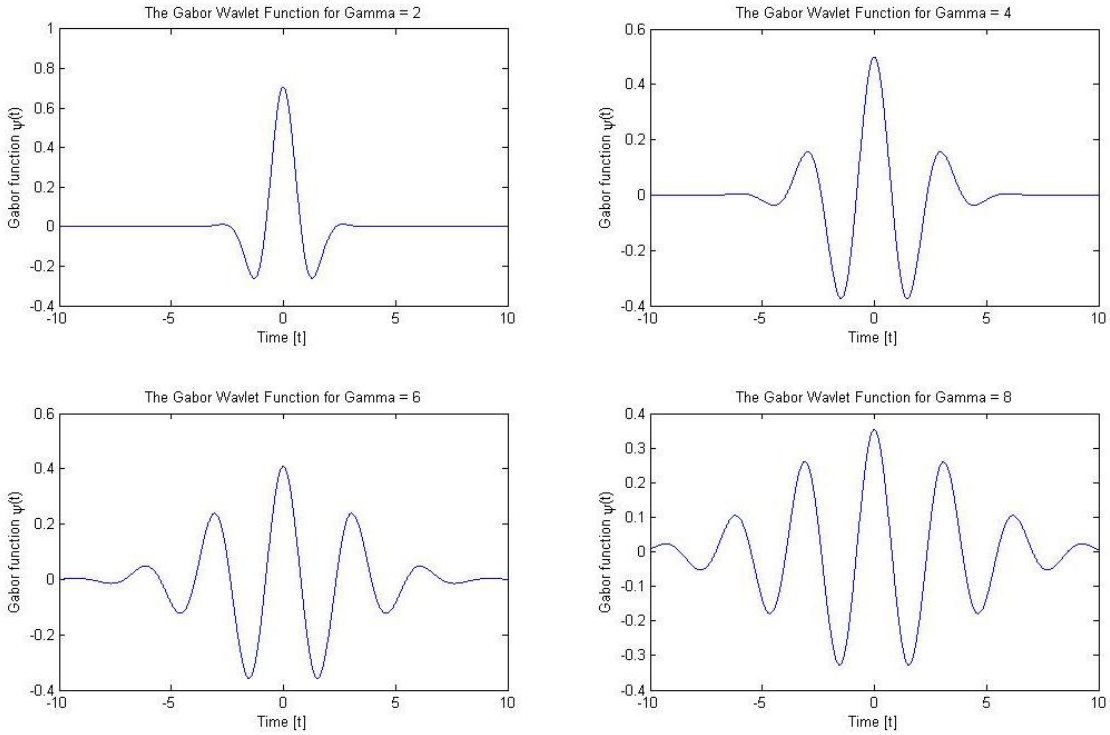

Figure 5. Gabor wavelet function with a = 0.5 and γ = 2, 4, 6, and 8

The γ also affects the time-frequency resolution of the Gabor Wavelet Transformation (GWT). Figure 6 shows a sine function with three different frequencies occurring at different time instances. For $\gamma = 1$ the resolution in frequency is immensely deteriorated as seen in the top left graph in Figure 7, whereas the change in time step is depicted clearly. But for γ = 28 the resolution becomes opposite. The bottom right image of Figure 7 shows that the time resolution is low as the time overlaps, while the frequency resolution is very sharp and clear. Hence there is a limited range of the γ values that can be used to reach a proper balance between the time and frequency resolutions.

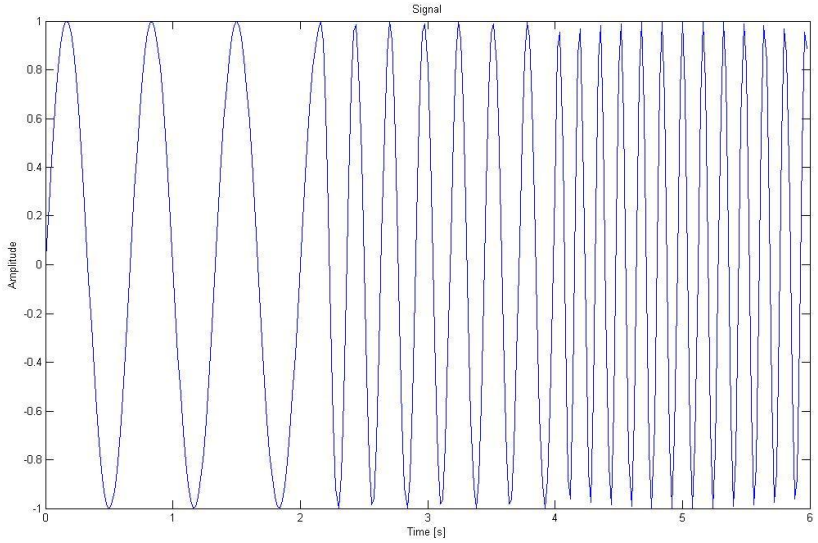

Figure 6. Sine signal with different frequency at different instance

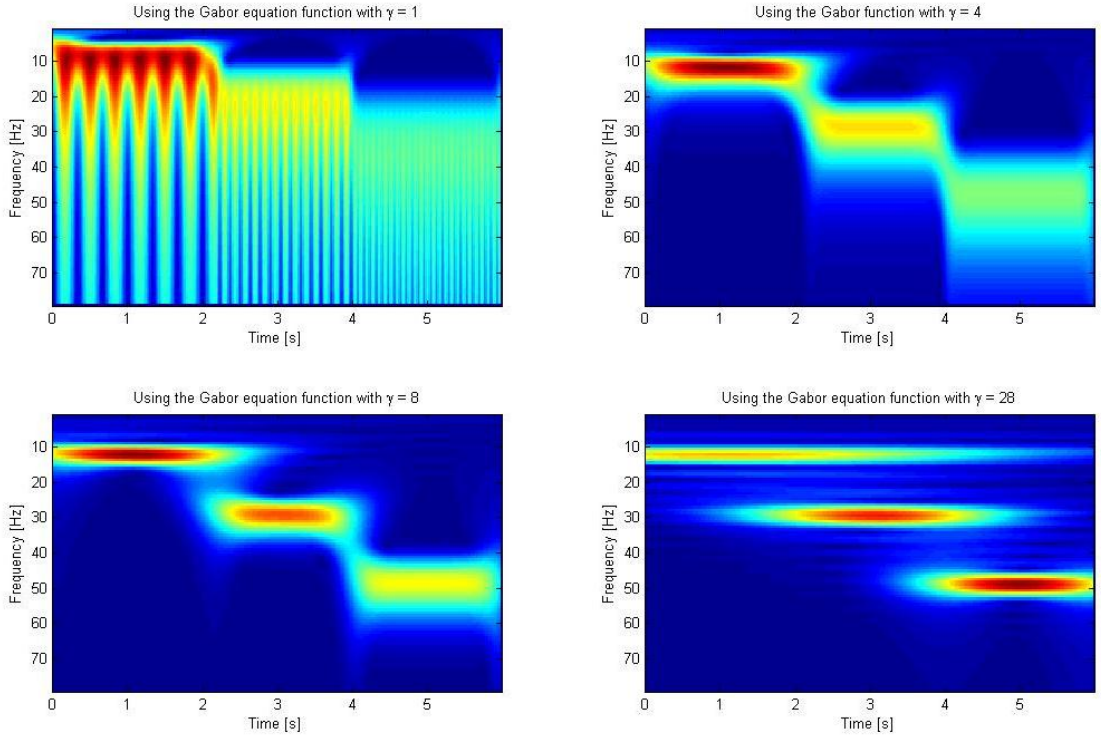

Figure 7. Effect of γ on GWT resolution γ used in the four images is 1, 4, 8, and 28.

3.3. Dispersion and Attenuation

Waves that deform when travelling through a medium are called dispersive waves. Attenuation factor 'Q' is defined to quantify the amount of deterioration of a dispersive wave as it propagates in time. These properties are a function of frequency. Since the traditional Fourier transform is not applicable for measuring the above property, frequency coefficients of the GWT are used. Ref. [33] mentions various factors of attenuation of Lamb waves:

- geometric spreading;
- material damping;
- dissipation into adjacent media; and
- wave dispersion.

As mentioned in [30] the logical way to measure attenuation factor is to compare the amplitude of the same wave forms at two different spatial locations. Hence if there are two locations on a specimen x_1 and x_2 in the same line of propagation of the wave where $x_1 > 0$ and $x_2 > 0$, the wave amplitudes at the two locations can be defined as

$$\boldsymbol{A_1} = \boldsymbol{A} * \mathbf{exp}(-\boldsymbol{k x_1}) \tag{13}$$

$$\boldsymbol{A_2} = \boldsymbol{A} * \mathbf{exp}(-\boldsymbol{k x_2}) \tag{14}$$

Therefore the attenuation, *Q*, is defined as

$$\boldsymbol{Q} = \frac{\boldsymbol{A_1}}{\boldsymbol{A_2}} = \mathbf{exp}(-\boldsymbol{k}(\boldsymbol{x_1} - \boldsymbol{x_2})) \tag{15}$$

3.3.1. Attenuation Factor – Q

Since the above equations are for single frequency component wave, and waves in materials such as NFC can carry multiple frequencies, therefore, GWT is used to decompose a wave into individual frequencies. Once the GWT is performed, the value of the maximum Gabor coefficient is found for a particular frequency along the time axis. The maximum value of the Gabor wavelet coefficients is denoted as $G_1(\omega)$ for that particular frequency and the corresponding time is noted as t_1. These values are used to calculate the attenuation factor and group velocity of the wave propagated. Figure 8 shows a visual for finding the Gabor wavelet coefficients.

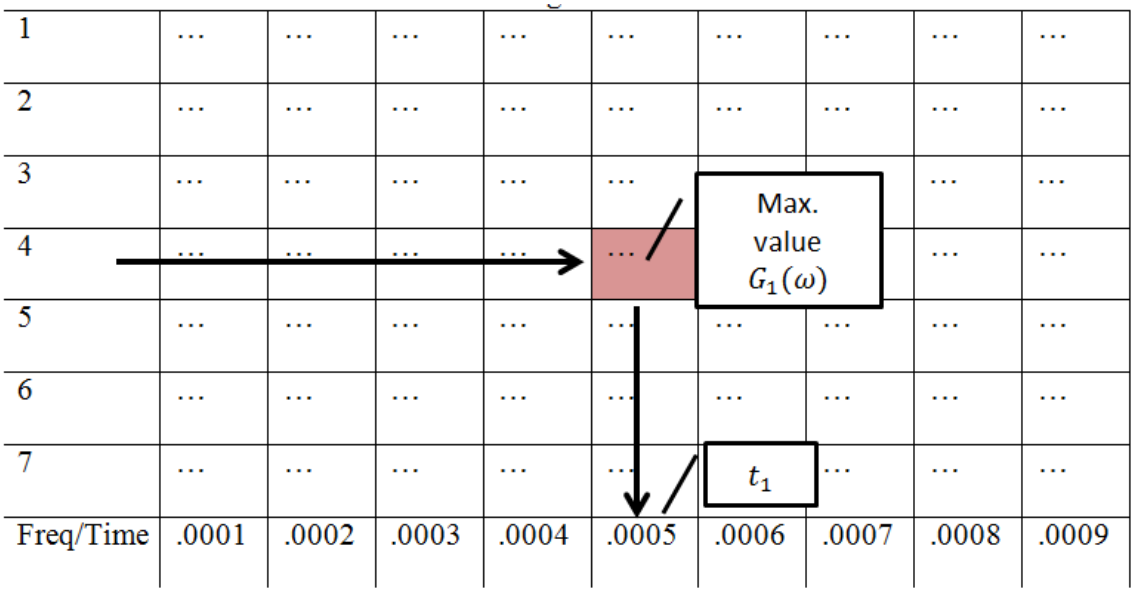

Figure 8. Chart showing how to find the maximum Gabor coefficient and the corresponding time for a particular frequency.

The Gabor wavelet coefficients are recorded for two different locations in the same line of the wave propagation and for the same frequency component. Let's assume that $G_1(\omega)$ and $G_2(\omega)$ are two different coefficient values of the same frequency

measured at two different locations, x_1 and x_2 with the distance d apart. Therefore the attenuation factor, Q, can be defined as a function of frequency and distance in decibel (dB) as

$$\boldsymbol{Q\ (dB) = \ -20log\frac{G_1(\omega)}{G_2(\omega)}} \tag{16}$$

3.3.2. Extraction of Dispersion Curves

The extraction of the dispersion curve requires the same procedure as mentioned above. Once the GWT is performed on the waveforms acquired at two different locations which is separated by distance *d*, the time corresponding to the maximum Gabor wavelet coefficients for a particular frequency indicates the arrival time of that particular frequency wave at that location [34]. Lets say for a particular frequency component ω at positions A and B, the corresponding time observed are $t_A(\omega)$ and $t_B(\omega)$, respectively, then the time taken for that frequency component to travel the distance *d* is given by

$$\boldsymbol{\Delta t(\omega) = \ t_B(\omega) - \ t_A(\omega)} \tag{17}$$

and the group velocity is therefore given by

$$\boldsymbol{v_g = \frac{d}{\Delta t(\omega)}} \tag{18}$$

Once the group velocity is obtained for each frequency component, the group velocity is then plotted against the frequency. The curve thus obtained is known as the dispersion curve.

4. MATERIALS, PREPARATION AND TESTING

This natural fiber composite research uses hemp fibers acquired through Hemp Traders and LLDPE (linear low density polyethylene) was obtained from TDL Plastics. The polymers were in a form of pellets of approx. 0.1 in diameter. The melting temperature of the pellets was 127^{O}C. The chemicals obtained were NaOH (obtained locally); while Toulene and MA-g-PE was acquired from Sigma Aldrich.

4.1. Fiber Modification and Treatment

The acquired fibers were approximately 10mm on average. In order to have better blend and dispersion of the materials, the fibers were soaked in liquid nitrogen and later grinded in a grinder to achieve finer and small fibers. Figure 9 shows the original fibers obtained from the supplier whereas the grinded fibers are shown in Figure 10.

Figure 9. Original fiber obtained

Once the fibers were grinded, the fibers were separated into three different batches; namely, untreated, NaOH treated, and MA-g-PE treated.

Figure 10. Grinded fiber using liquid nitrogen

Untreated Fiber: The grinder fibers were then dried in convection oven at $60^{O}C$ for 3-hour to reduce the moisture. Later the untreated fibers were further divided into three separate batches to mix with LLDPE in 10%, 20% and 30% vol. fraction.

Alkaline Treatment: NaOH pellets were dissolved in distilled water to create a 5% aqueous solution. The grinded fibers were soaked in 5% solution for 3-hour in room temperature. Later they were oven-dried at $60^{O}C$ for 3-hour and air dried for 24 hours. Once dried, the fibers were then again separated in three batches to mix with LLDPE in 10%, 20% and 30% vol. fraction.

Maleic anhydride treatment: Maleic anhydride grafted polyethylene pellet was mixed in toluene to create a 0.5% solution in 1-liter of toulene. The pellets were stirred until they were completely dissolved. The fibers were soaked in the solution for 3-hour. The drying and batching process of the fibers were followed similarly as mentioned above.

4.2. Composite Fabrication

The fibers and the polymers were divided in 10%, 20%, and 30% vol. Each batch was approximately 25cc in volume that was melt mixed in a HaakeBuchler compounding machine – Rheocord system 40. Figure 11 shows the image of the compounding machine used. At 50rpm, the batch was melt mixed for 3-min at a temperature of 150°C.

Figure 11. Haake compounding machine

Figure 12 shows the lumps of composite formed by the melt mixing process. These lumps were then compressed molded to form specimen planks (Figure 13) of the sizes mentioned in Table 3. The composite was then compressed molded in a Dake Compressing machine at a pressure of 800Pa for 10 minutes. Figure 14 shows the image

of Dake Compressing machine. The mold was manufactured in-house to create composite planks to cut into test specimen size.

Figure 12 The lump of composite formed from one batch of melt mixing from the compounding machine.

Figure 13 Plank of compressed composite from compression molding

Table 3 Size of specimens

Specimen size	Plank	Specimen size
Tensile	100 x 12.7 x 17.5 mm^3	100 x 12.7 x 3.5 mm^3
Flexural	64 x 12.7 x 16.25 mm^3	64 x 12.7 x 3.25 mm^3
Impact	--	D = 241.3mm, T = 2.54mm

Figure 14. Dake compression machine

4.3. Composite Static Testing

To determine the mechanical properties of the composite, two tests were employed. The density of the composite was also measured using Archimedean principal. The detailed experimental procedures are measured below in the subsections.

4.3.1. Tensile Test

Tensile test was performed referring to ASTM 3039 standard. The test was performed on Instron 5567 machine shown in Figure 15. The fabrication of the specimens has been mentioned above. The specimens were divided into three separate batches with fiber volume fraction of 10%, 20% and 30%. The fibers were randomly orientated during the fabrication, hence referring to the ASTM standard for tensile testing the size of the specimens were determined as follows - 100 x 12.7 x 3.5 mm^3 each. Five specimens were used for each volume fraction. Also there were no tabs used as mentioned in the standards. The gauge length was 64mm with the grip length of 18mm on each side and the crosshead of 5mm/min. The extension of the specimen was measured by the load-cell, and the gauge length was used to calculate the strain. The data points for the force and cross-head displacement were generated from the load cell into excel file.

The tensile stress and strain was calculated using the following equation.

$$\boldsymbol{\sigma_i} = \frac{\boldsymbol{F_i}}{\boldsymbol{A}} \tag{19}$$

$$\boldsymbol{\varepsilon_i} = \frac{\boldsymbol{\delta_i}}{\boldsymbol{L_g}} \tag{20}$$

where F_i: Force at i-th point, $\sigma_i$is the stress at the i-th point, A is the Area of the cross-section, ε_i is the Strain at the i-th point, δ_i is the displacement of the cross-head, L_g is the gauge length. The tensile modulus is measured from the linear stress-strain curve.

4.3.2. Flexural Test

The flexural test was performed following the ASTM D790 standard using the same machine. Five specimens were tested flat with a dimension of 64 x 12.7 x 3.25 mm^3 and the crosshead motion was 2mm/min. The support span was 50.8 with a span-to-depth ratio of 16:1. Figure 16 shows sample specimens. The stress at the middle of the specimen, and the elasticity of the modulus was calculated using the following equations:

$$\boldsymbol{\sigma_F = \frac{3PL}{2bd^2}} \quad (21)$$

$$\boldsymbol{E_b = \frac{mL^3}{4bd^3}} \quad (22)$$

where σ is the flexural stress, P is the vertical force, L is the length, b is the width of the specimen, d is the thickness of the specimen, m is the linear slope of the stress-strain curve, and E is the Elastic modulus.

4.3.3. Density Test

The density of HEMP-LLDPE was measured with reference to ASTM C20. Three specimens of different small sizes were used for each fiber volume fractions and treated fibers as the ASTM C20 uses large brick size specimen to measure density.

Figure 15 Tensile and flexural test performed on Instron 5567

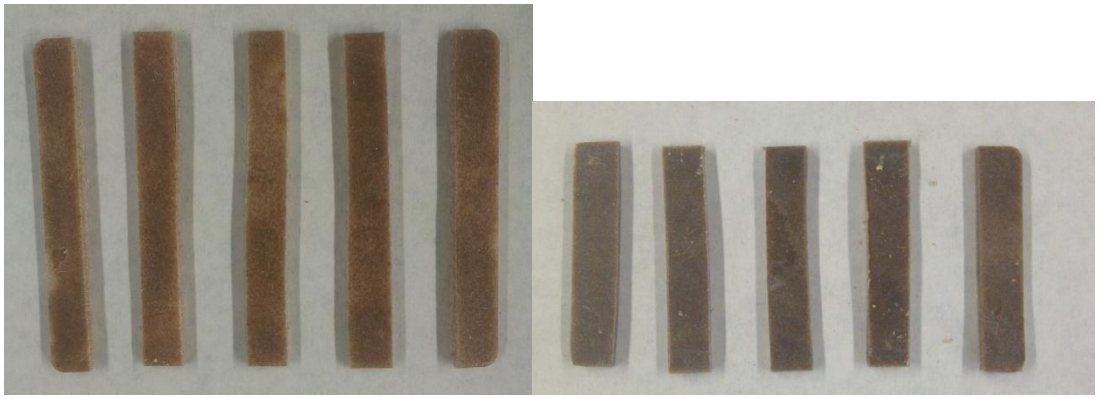
Figure 16. Specimens for tensile and flexural specimens

4.4. Composite Dynamic Testing

A thin disk specimen mentioned above has been used for the dynamic testing. The disk was divided in eight different directions as shown in the Figure 17. A dead steel ball of 200gm was dropped at the center of the disk to generate Lamb waves propagating outward. The ball was dropped from a height of 6" to impact with a 0.3J of energy. The waves were then sensed by two 2MHz, wedge transducers shown in Figure 18. The transducers were connected to a Tektronix TDS 2012B oscilloscope with a BNC cable.

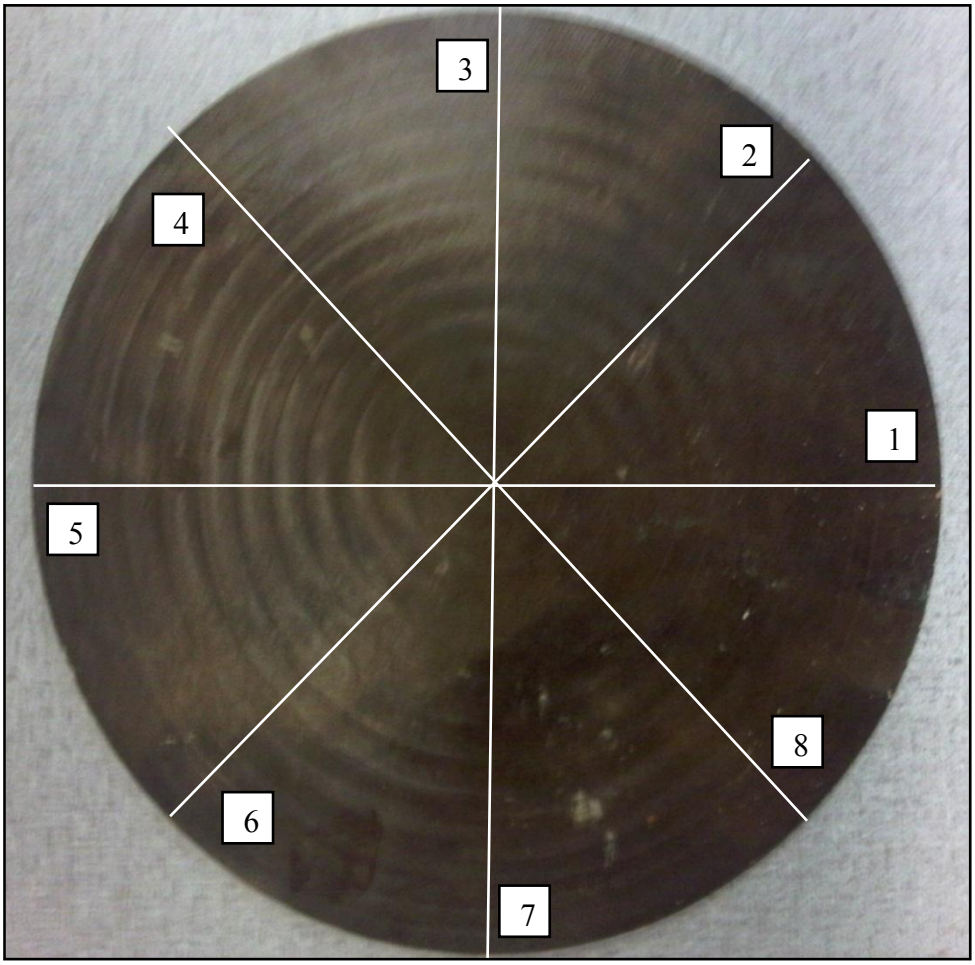

Figure 17. Disk specimen for impact testing with direction labeled.

Figure 18. 90° angle wedge transducers

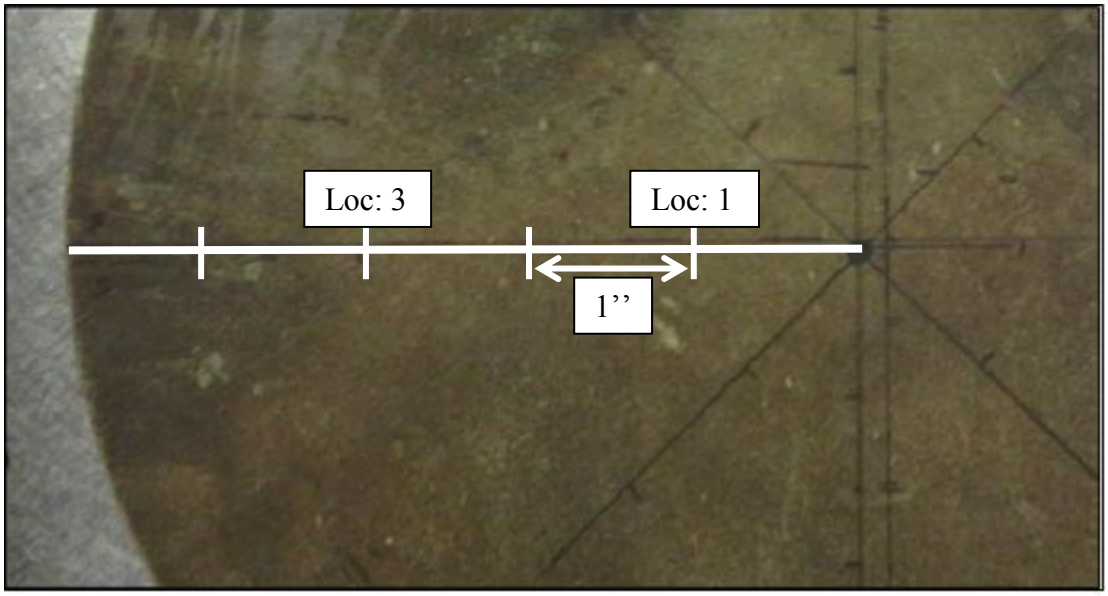

Figure 19. Location of transducers

The oscilloscope was connected to a computer with a Tex TDS 2012B – Openchoice desktop software. As it can be seen in Figure 19. Location of transducersthe transducers were placed in Loc (location) 1 and 3 with a 2" separation between them.

In the second experiment, three real type defects were artificially created in the specimen. These defects were inflicted at 2.5" from the center as shown in Figs. 20-22. They were

1. a dent along direction 1,
2. a quarter inch hole along direction 2, and

3. a series of shallow scratched along direction 3.

The transducers were placed at the same location 1 and 3 to acquire the waves. Once the waves were acquired they were processed using GWT. Attenuation factor, group velocity and the GWT image were extracted. Post damage data were then compared with damage-free data to analyze the difference.

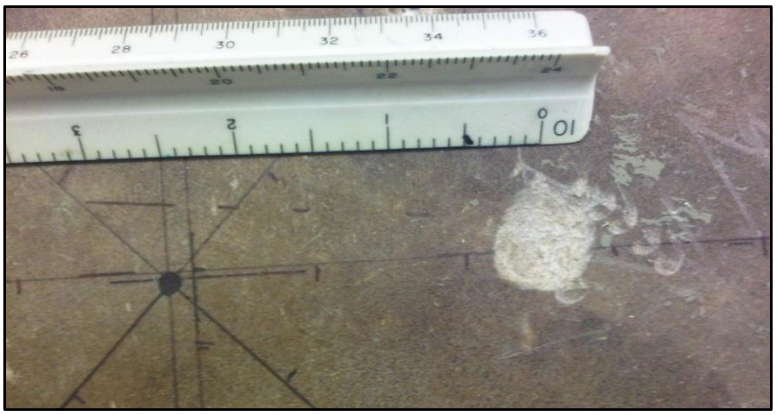

Figure 20. A dent along direction 1

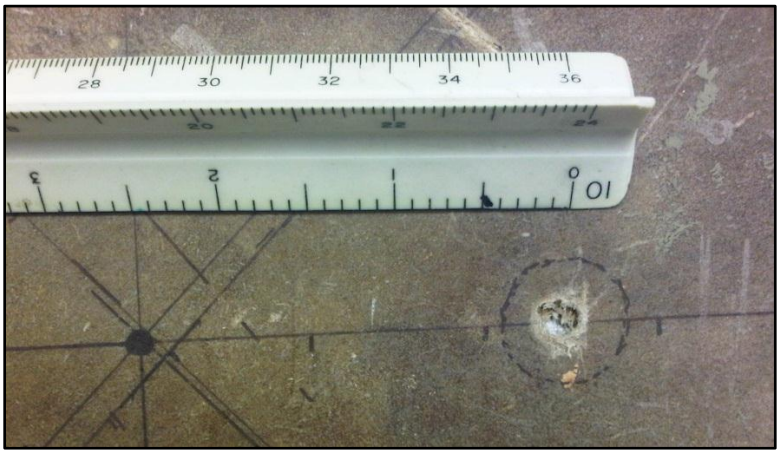

Figure 21. A quarter inch hole along direction 2

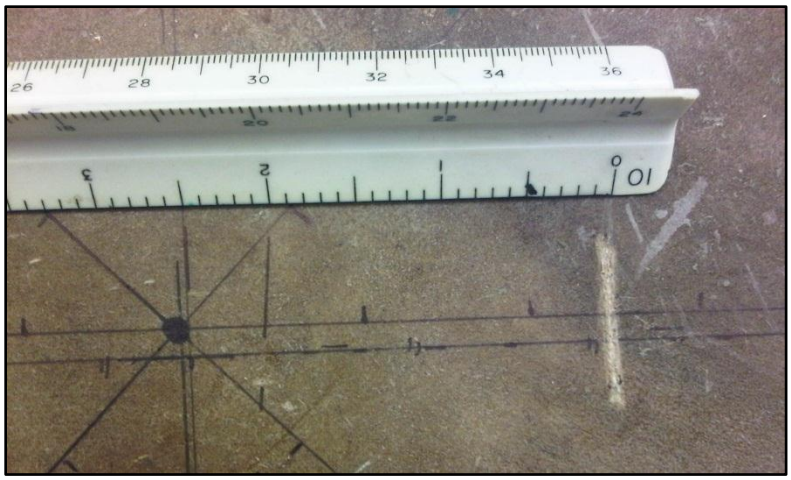

Figure 22. A shallow scratch to depict cracks in direction 3

4.5. Experimental Errors

Experimentation requires a precise approach and accurate methods to obtain proper results. Any disorganized approach can produce errors in the data obtained. Despite of following impeccable procedures; errors and glitches could still be inevitable during experimentation. As mentioned earlier, the natural fibers are hydrophilic in nature having a high tendency of absorbing moisture. The fibers and specimens were exposed to air at various instances that may have resulted in moisture absorption. During the surface treatment, the fibers were treated with several chemicals; though the fibers were dried in the oven, it was uncertain if the fibers were completely moisture-free. Fibers with moisture could result in degradation of material properties, improper adhesion between the fiber and matrix.

After the melt mixing of the fibers and the polymers, the composite specimens were created using compression molding. The die that was made in-house had tool

marks which were imparted during the machining of the die. A professionally manufactured fitting die can create better specimens with uniform thickness.

Lamb waves are very sensitive to geometric shape and interference. There were several errors and estimations occurred during the experimentations that could have compromised the waveform data and associated results. During the impact testing, the thin disk-type specimen was impacted with a dead steel ball at the center of the disk and the transducers were placed at location 1 and 3 (Figure 17). Though the ball was aimed to be dropped precisely in the center, there were certainties that the exact location of impact on the specimen may not have been accurately the same when acquiring data for all directions. A slight difference in impact location would have created different waveforms. Therefore it is suggested to device a mechanism using a rotatory motion that would apply an impact at the exact location. The device should be able to alter the imparting impact energy as well.

The transducers used in this research were a 90° angle beam wedge shown in Figure 16. Due to the dimensions of the wedges there are approximations and errors involved. The wedges were 0.5" thick and the sensor averaged the propagating waves. While acquiring the data in different directions, there were constantly being mounted and dismounted. This may have also generated errors in for example the distance between the two wedges and the precise positing of the wedges (perpendicular to the propagating waves). An alternate solution could be using non-contact optical sensors such as laser interferometers.

Ideally, the best method would be to use PZT transducers embedded in all the locations where the waveforms must be acquired. The PZTs should be connected to a Data Acquisition (DAQ) card with the DAQ connected to the other peripherals such as a computer or an oscilloscope. Employing a method facilitates the acquiring of data with one impact in all directions and from all locations. This procedure can minimize various errors due to triggering; it would eliminate the procedure of mounting and dismounting transducers. It was also observed that after repeating the impact several times, there was a slight deformation at the center, hence using the above method can avoid such an issue.

5. RESULTS AND DISCUSSION

5.1. Effect of Surface Treatment on Static Properties

This chapter talks about the effects of the various surface treatments on hemp fibers and influence of such treatments on the composite properties. The comparison is done among three different types of fiber composites – untreated (UNHEMP), sodium hydroxide treated (NAHEMP) and MA-g-PE treated (MAHEMP). Each fiber composite have a fiber volume fraction of 10%, 20% and 30%.

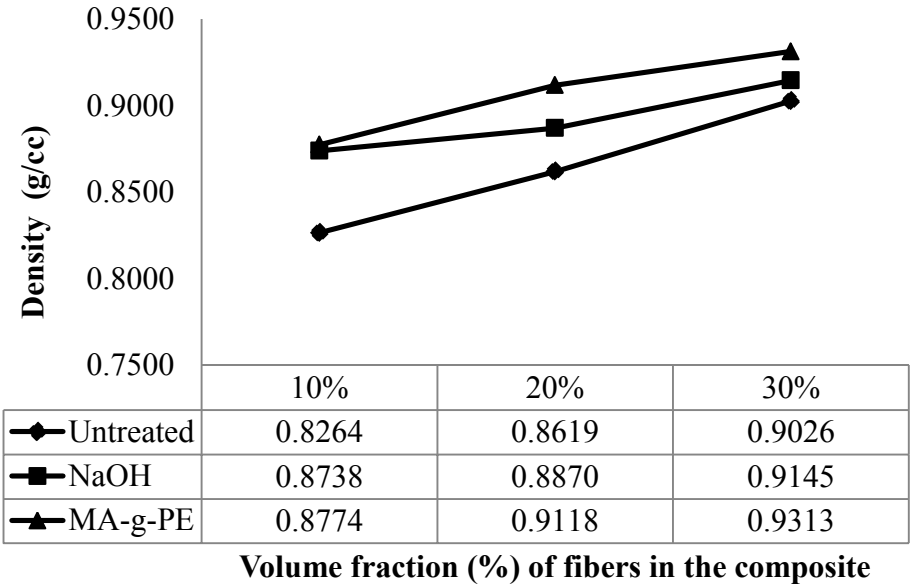

	10%	20%	30%
Untreated	0.8264	0.8619	0.9026
NaOH	0.8738	0.8870	0.9145
MA-g-PE	0.8774	0.9118	0.9313

Figure 23. Density of UNHEMP, NAHEMP and MAGHEMP composites

5.1.1. Density

Figure 23 shows the density comparison of the composites. 10% vol. of the UNHEMP shows the lowest density of 0.8264g/cc. It is observed that the surface treatment increases the density of the composites. 30% vol. of the MAGHEMP composite recorded a density of 0.9313g/cc. The increase in density implies that the

water molecule from the cell-wall have been displaced with the compound ions to make the fibers heavier. Therefore any form of surface treatment of the fibers increases the density of the composite. Table 4 shows a comparison of statistical data of the density of UNHEMP, NAHEMP and MAHEMP composites. It shows the Average values, Standard deviation and covariance percentage of three tested samples for each category in each fiber volume fraction. Table 4 shows a statistical representation on the values of the density of these composites.

Table 4 Statistical comparison of UNHEMP, NAHEMP and MAHEMP composite density

UNHEMP	**10%**	**20%**	**30%**
Average	0.8264	0.8619	0.9026
Std. Dev	0.0657	0.0318	0.0235
CV (%)	7.9511	3.6948	2.6083

NAHEMP	**10%**	**20%**	**30%**
Average	0.8738	0.8870	0.9145
Std. Dev	0.0274	0.0150	0.0291
CV (%)	3.1392	1.6891	3.1779

MAHEMP	**10%**	**20%**	**30%**
Average	0.8774	0.9118	0.9313
Std. Dev	0.0235	0.0227	0.0209
CV (%)	2.6784	2.4854	2.2462

5.1.2. Untreated Composite

The untreated HEMP fiber with LLDPE reported the following stress and strain curve for 10%, 20% and 30% vol. fraction in Figs. 24-26.

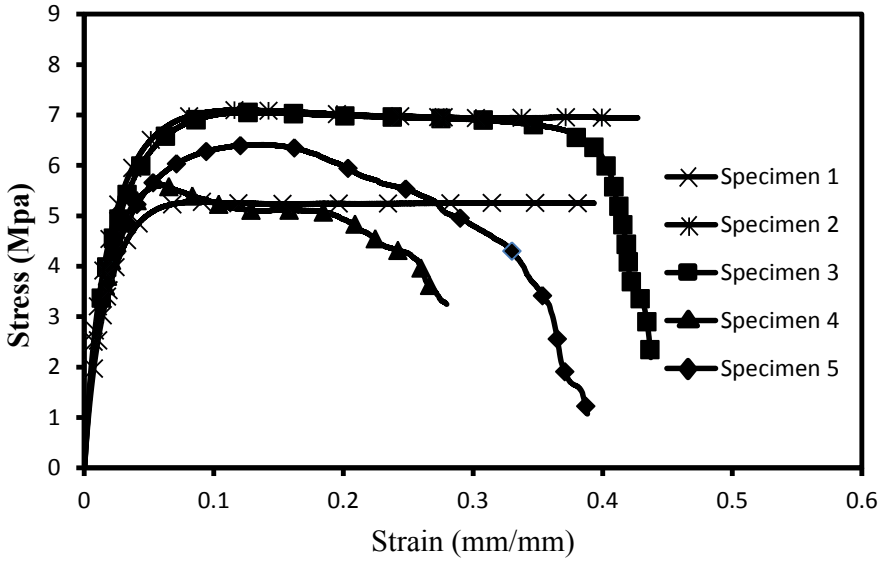

Figure 24 Stress-strain curve of 10% Vol. of UNHEMP

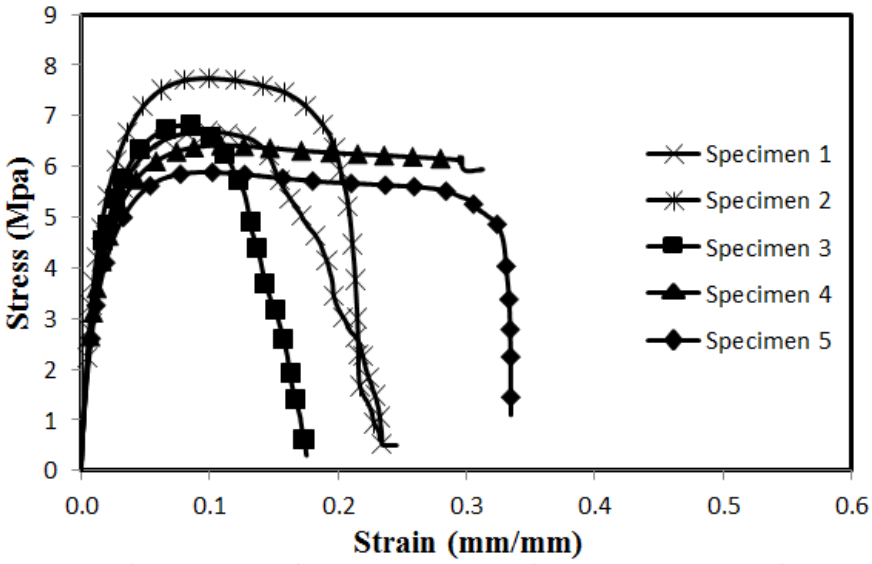

Figure 25. Stress-strain curve for 20% vol. of UNHEMP

It can be seen from Figs. 24 and 25 that they have high strain at failure when compared to Figure 26. It is precisely due to the low percentage of fiber and higher amount of polymer in the specimen. Figure 26 shows lower failure strain as it has high fiber fraction. It is also observed the stress-strain curve of all the specimens for 30% vol. fraction are close to each other.

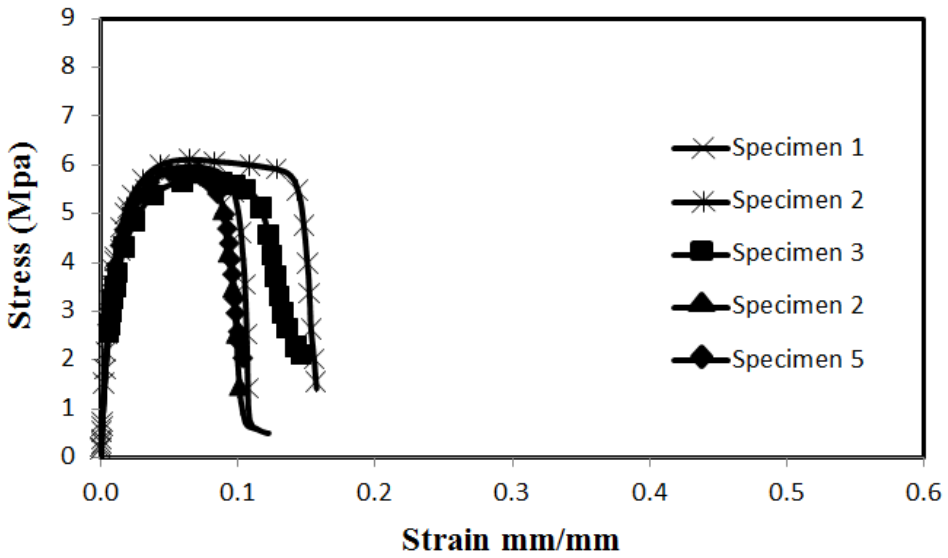

Figure 26 Stress-strain curve of 30% vol. UNHEMP

Table 5 Tensile strength and tensile modulus of UNHEMP of five samples

UNHEMP	**Tensile Strength (MPA)**			**Tensile Modulus (GPA)**		
	10%	20%	30%	10%	20%	30%
Average	6.2900	6.7100	6.0020	0.3116	0.4218	0.5302
Std Dev.	0.8262	0.6759	0.1054	0.0395	0.0380	0.0446
CV (%)	13.1356	10.0742	1.7569	12.6726	9.0159	8.4162

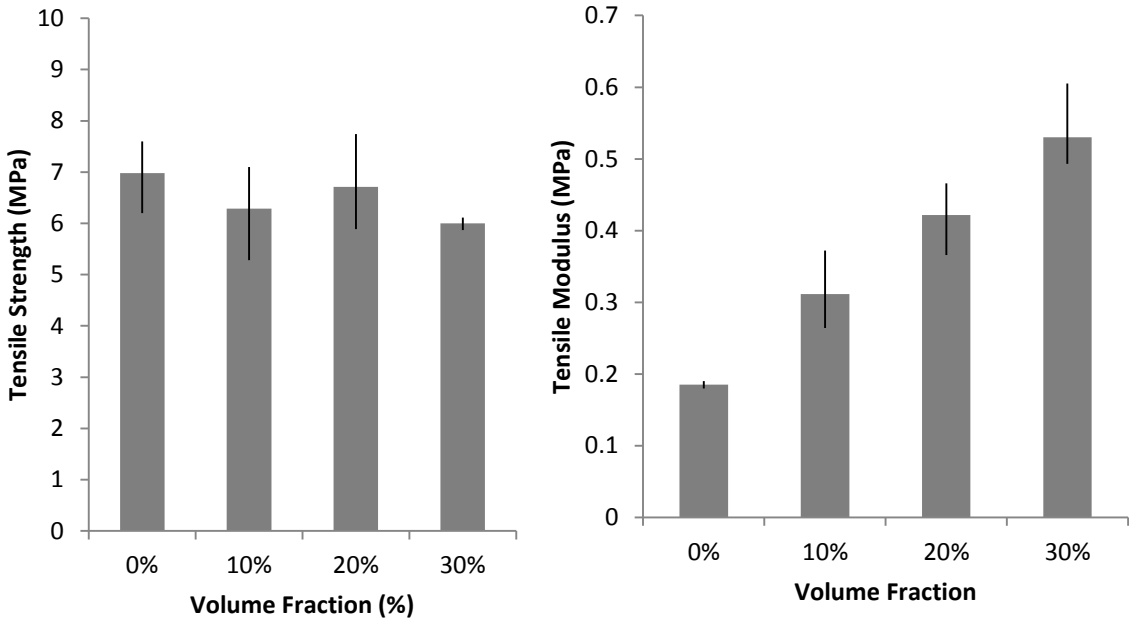

Figure 27. Tensile strength and modulus of 10%, 20% and 30% UNHEMP

Table **5** shows the summary of ultimate strength and young's modulus of the UNHEMP. It can be inferred that the tensile strength at 30% vol. fraction has extremely low co-efficient of variance (CV) but at other vol. fraction the CV is high. Table 6 shows the flexural strength and flexural modulus values of all the specimens and their SD and CV. 20% UNHEMP has the lower SD and CV compared to the other volume fraction.

Figure 27 shows the tensile strength and modulus values of 10%, 20% and 30% UNHEMP composites. It can be seen that the tensile modulus increase moderately as the volume fraction of the fiber increases in the composite. Whereas, the tensile strength values are little erratic. The inclusion of the fibers in the polymer does not really shows any significant increase or decrease.

Table 6 Flexural strength and flexural modulus of UNHEMP of five samples

UNHEMP	Flexural Strength			Flexural Modulus		
	10%	20%	30%	10%	20%	30%
Average	7.6360	8.9060	10.6320	0.2568	0.3290	0.4128
Std. Dev.	0.6225	0.4850	1.1939	0.0338	0.0370	0.0612
CV	8.1524	5.4452	11.2296	13.1808	11.2544	14.8291

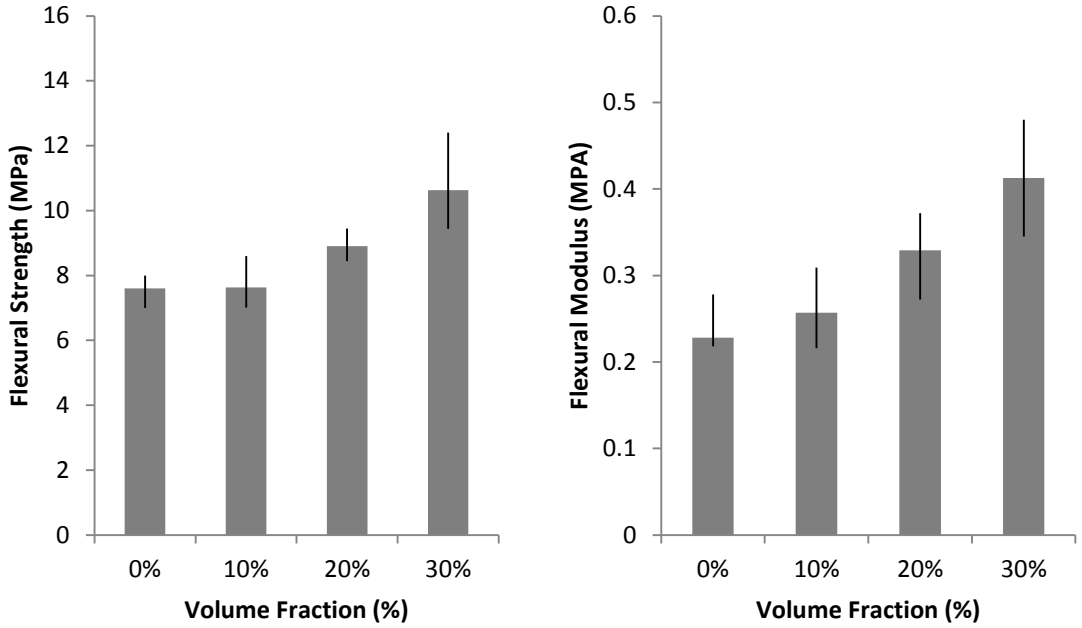

Figure 28. Flexural strength and modulus of 10%, 20% and 30% UNHEMP

Figure 28 shows the flexural strength and modulus of UNHEMP composite. The flexural values for UNHEMP show consistent results where the values increase with increasing volume fraction. Even though there are values overlapping among the fiber vol. fractions, the average values do show increments.

5.1.3. Alkaline Treatment

The chemical modification is used to optimize the adhesion between the fibers and polymers. The hydroxyl group in the cell walls gives the fibers a hydrophilic nature. As mentioned earlier these chemicals react with the cell wall of the fibers and remove the waxy substances and the hydroxyl group to perform a better adhesion.

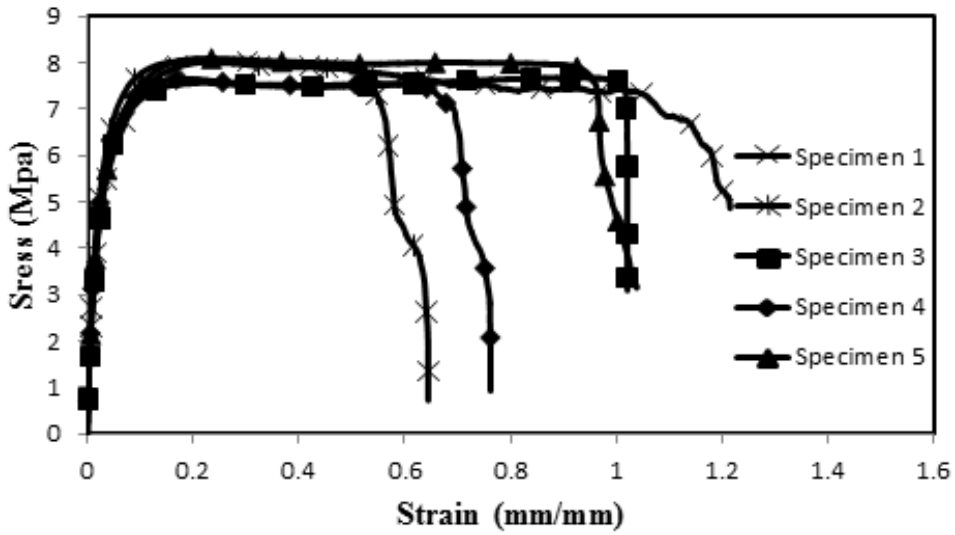

Figure 29 Stress-strain curve of 10% NAHEMP

Figure 29 shows stress-strain curve of 10% NAHEMP composite, it can be seen that the ultimate stress points of the all the curves are located close to each other, showing low SD for 10% NAHEMP, it can be verified in Table 7. Figure 30 shows the stress strain curve of 20% vol. fraction composite. The bottom figure shows an expanded view of the stress-strain curve where curves for each specimen can be distinguished. It can be clearly seen that the strain at failure for 20% is lower when compared with 10% vol. fraction. It can also be observed that there are large differences among the point of failure for the specimens for 10% and 20% vol. fraction.

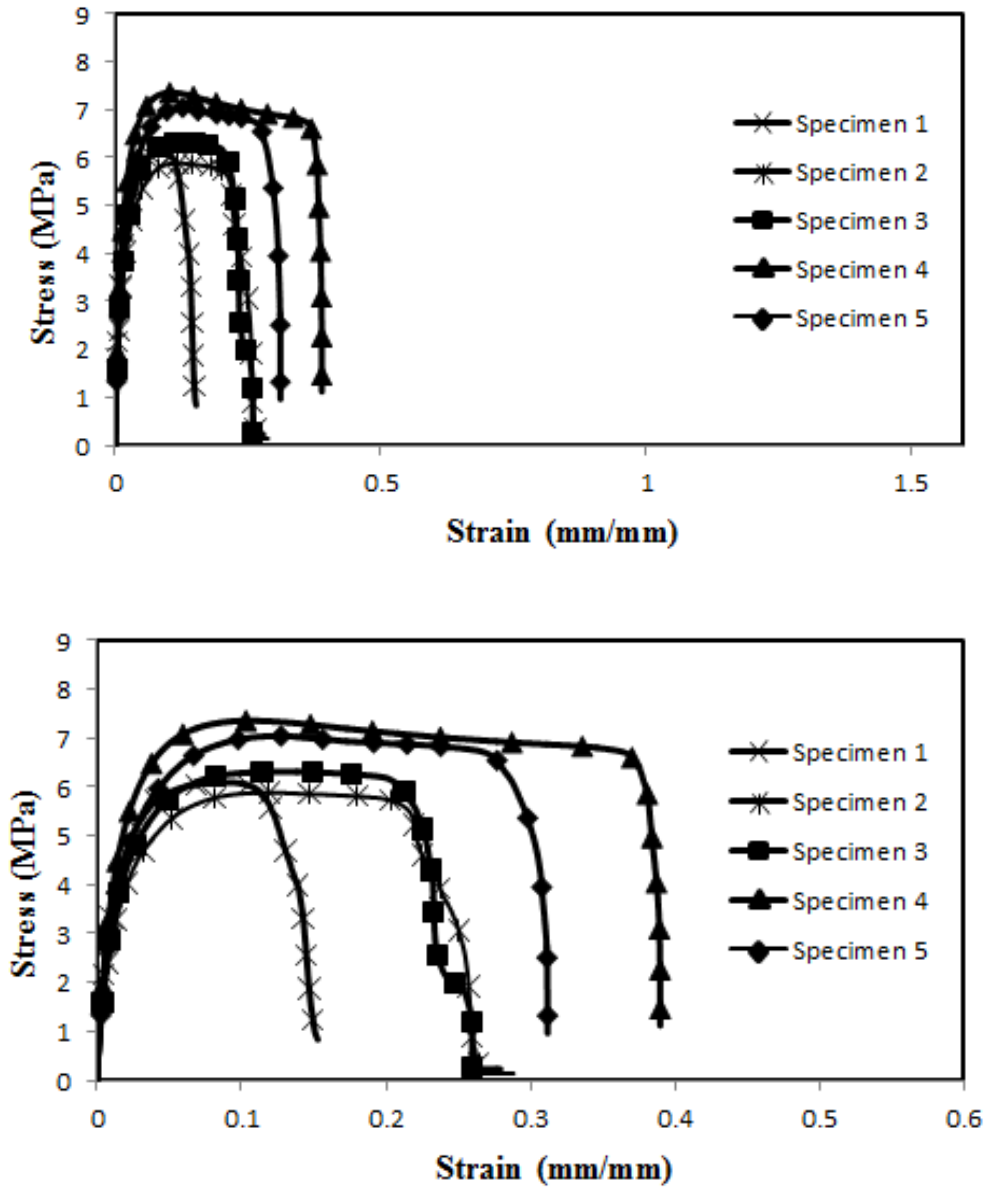

Figure 30 Stress-strain curve of 20% NAHEMP. Bottom graph shows an expanded view of the above graph with low strain values

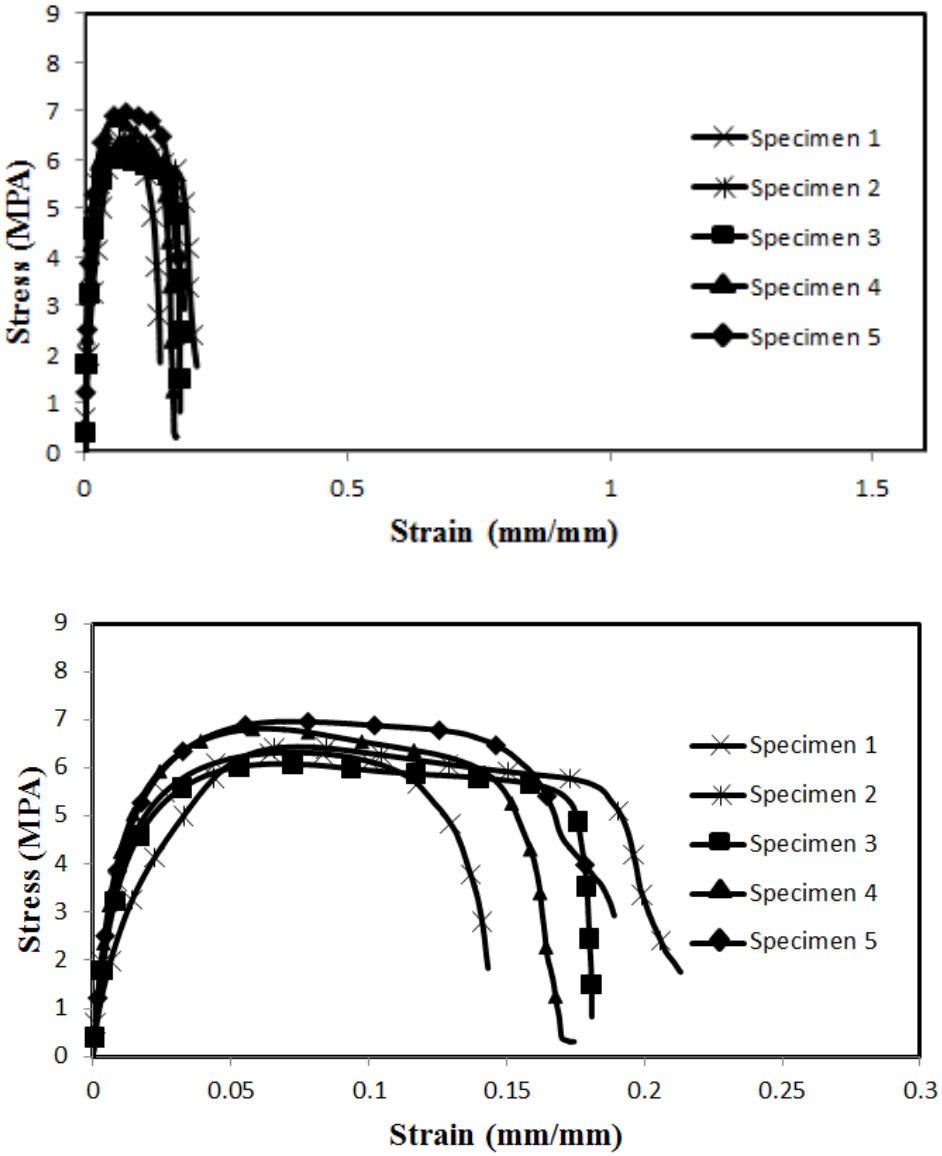

Figure 31 Stress-strain curve of 30% NAHEMP. Bottom graph shows an expanded view of the above graph with low strain values

Figure 31shows lower strain percentage at the failure compared to 10% and 20% NAHEMP composites. Table 7 shows the statistical values for the NAHEMP composites. It is observed that there is not much difference in the average values of

tensile strength for 20% and 30% volume fraction. The strength values decreases from with increase in fiber volume.

Table 7 Tensile strength and tensile modulus of NAHEMP of five samples

NAHEMP	Tensile Strength (MPA)			Tensile modulus (GPA)		
	10%	20%	30%	10%	20%	30%
Average	7.8780	6.5440	6.5400	0.3192	0.4360	0.6702
Std. Dev.	0.2548	0.6318	0.3647	0.0662	0.0579	0.0656
CV	3.2342	9.6554	5.5763	20.7317	13.2909	9.7919

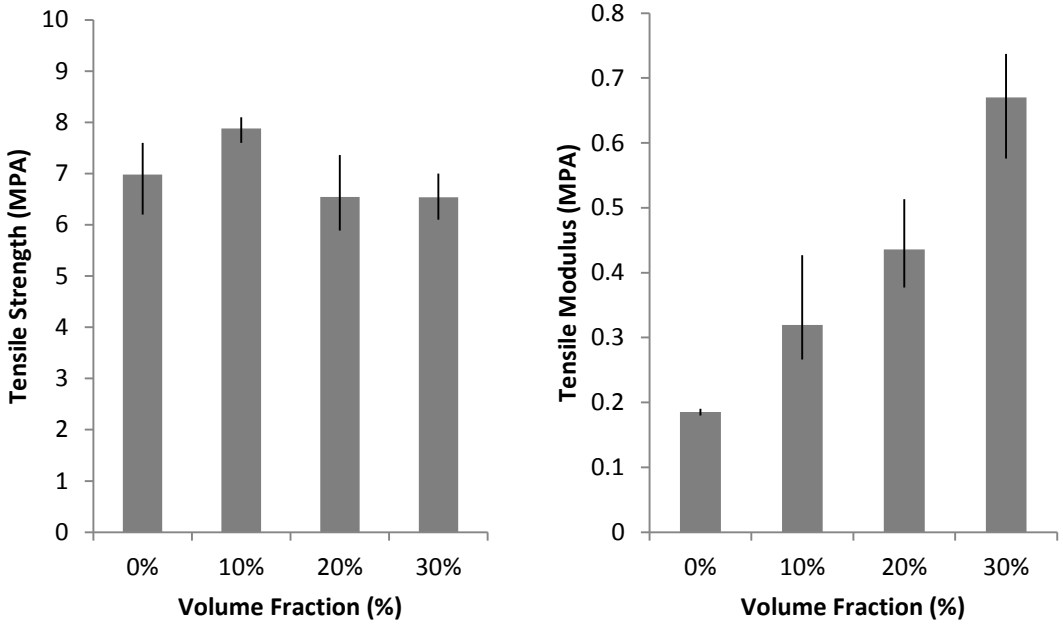

Figure 32. Tensile strength and modulus of 10%, 20% and 30% NAHEMP

Figure 32 shows the tensile strength of the composite with 10%, 20% and 30% vol. of fibers of NAHEMP composites. For 10% vol. of NAHEMP, a 25% increase in tensile strength is seen when compared to (Figure 27) the tensile strength UNHEMP for

10% vol. fraction. The tensile modulus of NAHEMP composite is found to be higher than UNHEMP for all the volume fractions considered.

Table 8 shows the summary for flexural values of all five specimens. The table shows low CV for flexural strength values showing the ultimate flexural strength to be close among all the specimens. The variation in flexural modulus is higher than flexural strength but have similar values not with a large difference when compared with flexural modulus of UNHEMP (Table 5).

Table 8 Flexural strength and flexural modulus of NAHEMP of five samples

NAHEMP	**Flexural Strength (MPA)**			**Flexural Modulus (GPA)**		
	10%	20%	30%	10%	20%	30%
Average	9.4000	11.4300	11.9840	0.3294	0.4882	0.5612
Std. Dev.	0.5813	0.5380	0.6937	0.0439	0.0835	0.0630
CV	6.1844	4.7073	5.7880	13.3344	17.1103	11.2250

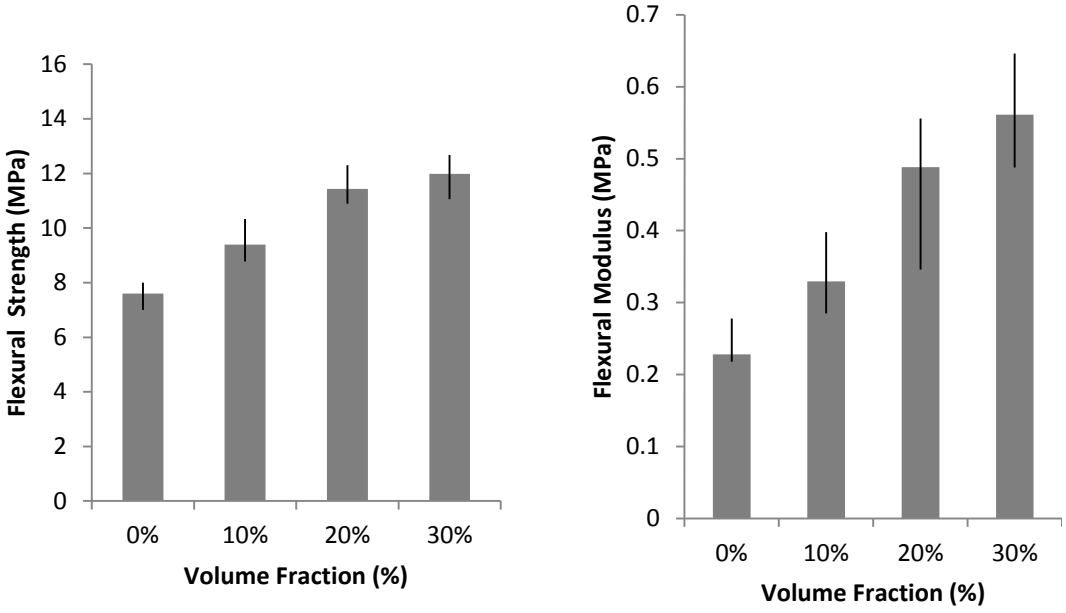

Figure 33. Flexural strength and modulus of 10%, 20% and 30% of NAHEMP

The alkaline treatment produced a significant improvement in the flexural strength and flexural modulus also. The values of flexural strength and flexural modulus for UNHEMP and NAHEMP composites are given in Figure 28 and Figure 33, respectively. 20% vol. of NAHEMP showed the highest percentage improvement in flexural strength by 28% when compared with 20% vol. UNHEMP recorded 8.9MPa while NAHEMP composite recorded 11.43MPa. Similarly the flexural modulus at 20% vol. showed the best improvement by 48%, whereas 30% vol. fraction showed only 36% improvement.

The results mentioned above prove that alkaline treatment improves certain properties of the composite. There are multiple of ways for NaOH to react with the fibers to achieve a better adhesion [4]

- The treatment increases the surface roughness of the fiber to have a better linking with the matrix.
- The fiber surface gets better cellulose exposure that increases the reaction sites with the matrix.

Hence the data prove that the usage of NaOH improves the fiber adhesion with the polymer, thus providing better properties than the UNHEMP composite.

5.1.4. Maleic Anhydride Treatment

Figure 34 show the Stress-Strain curve of MAHEMP composite. 10% volume fraction MAHEMP composites show 100% strain except for one specimen which was not tested properly. Figure 34 also shows high difference in the Tensile strength and the point of failure for each specimens. Table 9 shows the average value of tensile strength for 10% vol. fraction. The CV for 10% vol. fraction s is higher than 10% which shows higher differences in the tensile strength values for each specimen.

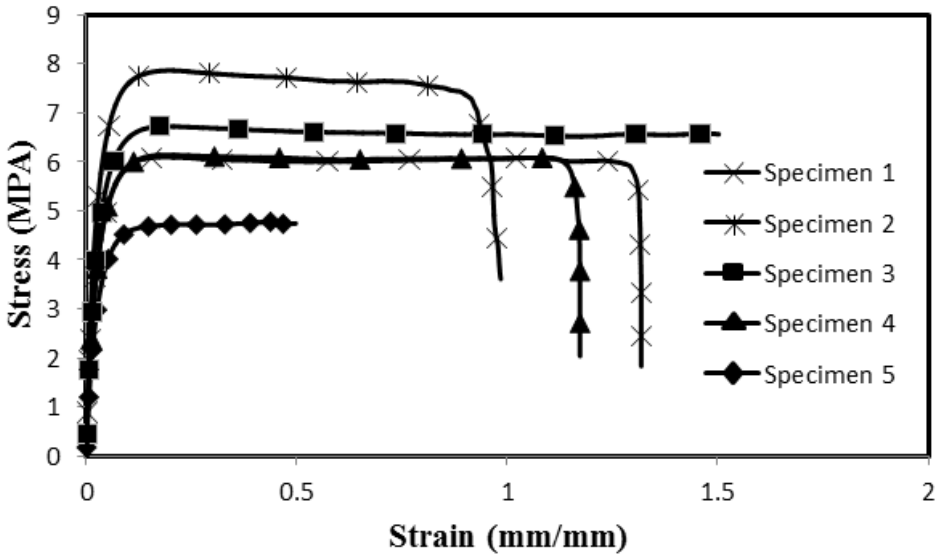

Figure 34 Stress-strain curve of 10% MAHEMP

Figure 35 show the stress-strain curves for 20% vol. fraction of MAHEMP composites. It is evident that the average values for strain at failure are very low when compared with 10% vol. fraction from the graphs. But despite having lower strain values at failure, there are high differences among the strain values at failure for each specimen. .Graphically it can also be observed that the stress-strain curves for all the specimens of 20% vol. fraction are closer compared to 10% vol. fraction

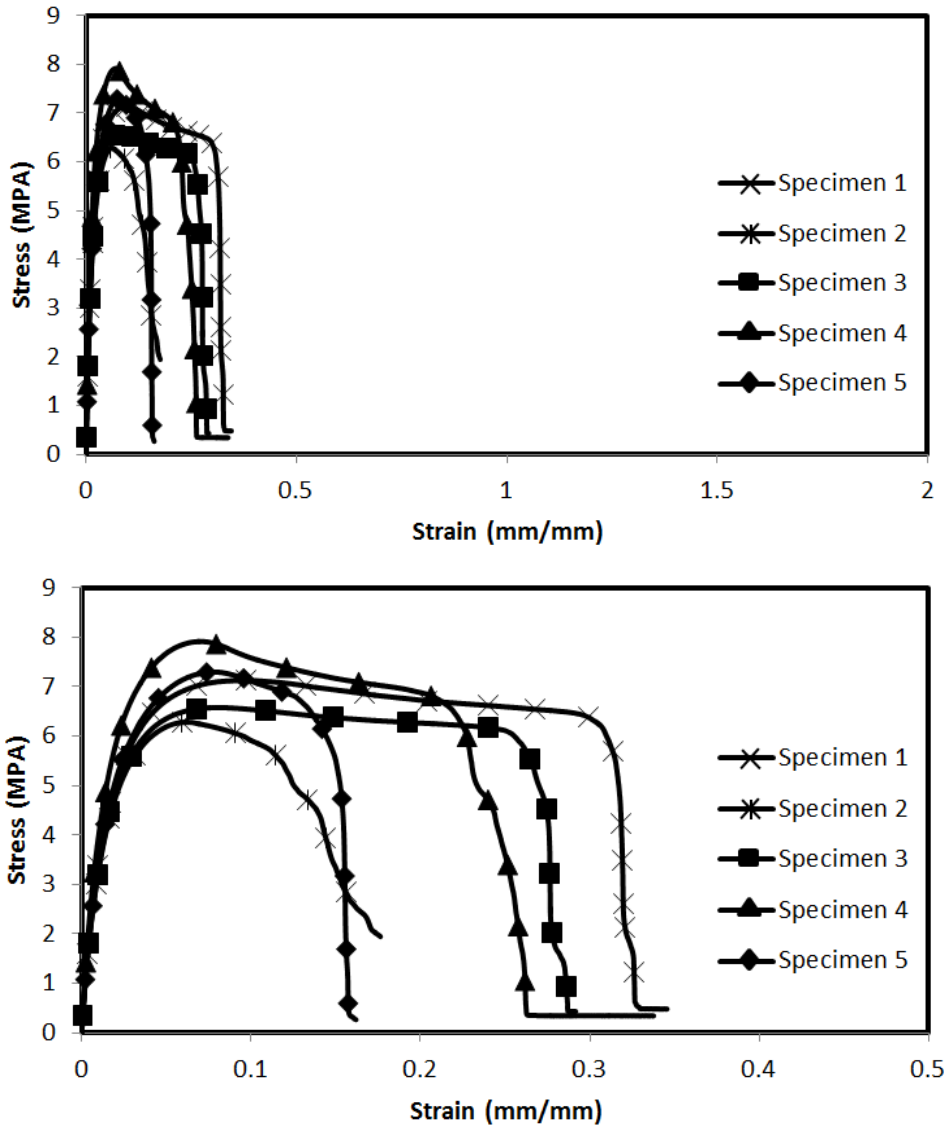

Figure 35 Stress-strain curve of 20% MAHEMP. Bottom graph shows an expanded view of the above graph with low strain values

Figure 36 shows the stress-strain curve for 30% vol. fraction MAHEMP composite. When compared with stress-strain curves for 30% vol. fraction of NAHEMP composites (Figure 31) it can be seen that the averages stain values at failure is lower compared to 30% vol. fraction. It can also be observed that with Ma-g-PE treatment the composites show less plasticizing effect i.e. in Figure 31 is can be seen that the curves

runs flat after reaching the ultimate strength point while for 30% MAHEMP composites (Figure 36), after reaching the ultimate stress point the curves decays fast to failure.

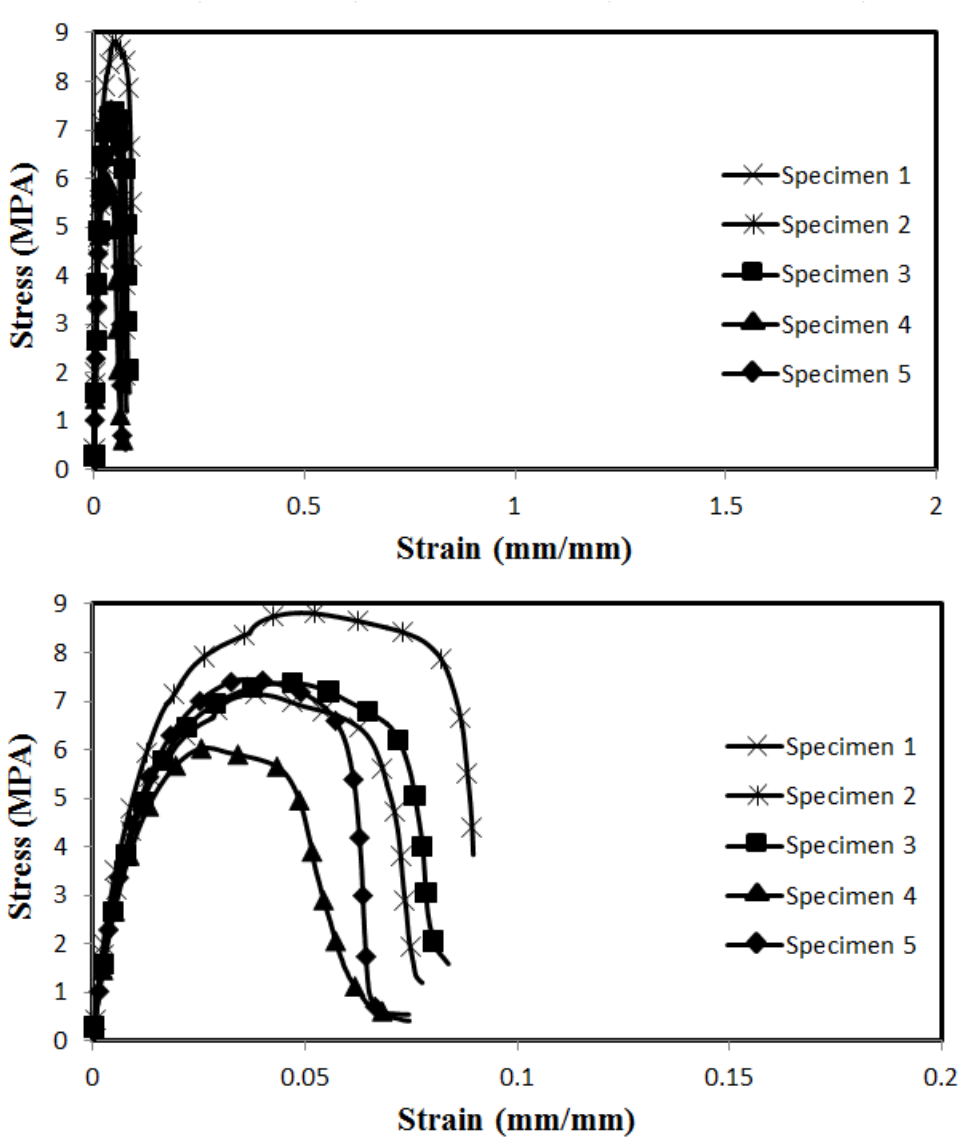

Figure 36 Stress-strain of 30% MAHEMP. Bottom graph shows an expanded view of the above graph with low strain values

Table 9 shows the statistical values for all vol. fractions for MAHEMP composites. The average values of the specimens for 20% and 30% vol. are higher than

UNHEMP and NAHEMP composites values and so are the values of CV for most vol. fractions.

Table 9 Tensile strength and tensile modulus of MAHEMP of five samples

MAGHEMP	Tensile Strength (MPA)			Tensile Modulus (GPA)		
	10%	20%	30%	10%	20%	30%
Average	6.3080	7.0314	7.3560	0.2392	0.4460	0.6754
Std. Dev.	1.0957	0.6396	0.9905	0.0634	0.0504	0.0966
CV	17.3697	9.0962	13.4651	26.4840	11.2990	14.3082

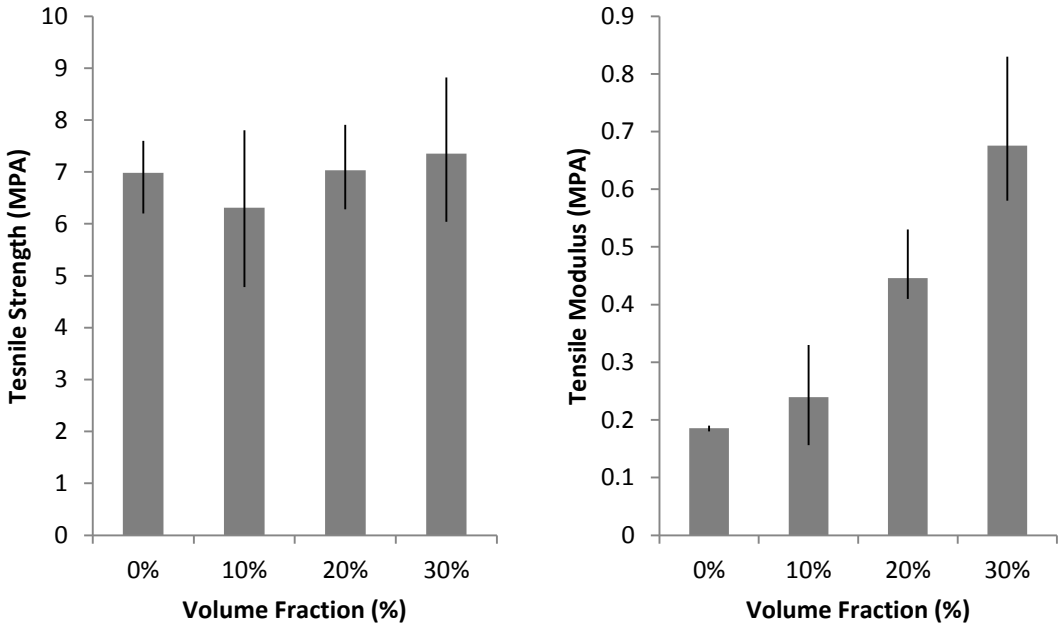

Figure 37. Tensile strength and modulus of 0%, 10%, 20% and 30% and MAHEMP

Figure 37 shows the tensile strength and modulus for MAHEMP composites. Similar to NAHEMP composites is can also be seen that tensile strength values of

different fiber volume fraction do not show significant differences. However, the tensile modulus shows promising increments as the fiber vol. fraction increases.

Table 10 Flexural strength and flexural modulus of MAHEMP of five samples

MAGHEMP	Flexural Strength (MPA)			Flexural Modulus (GPA)		
	10%	20%	30%	10%	20%	30%
Average	8.5220	11.3840	13.6600	0.2456	0.4406	0.6584
Std. Dev.	1.5372	0.6553	1.2482	0.0479	0.0486	0.2430
CV	18.0382	5.7564	9.1376	19.4943	11.0370	36.9017

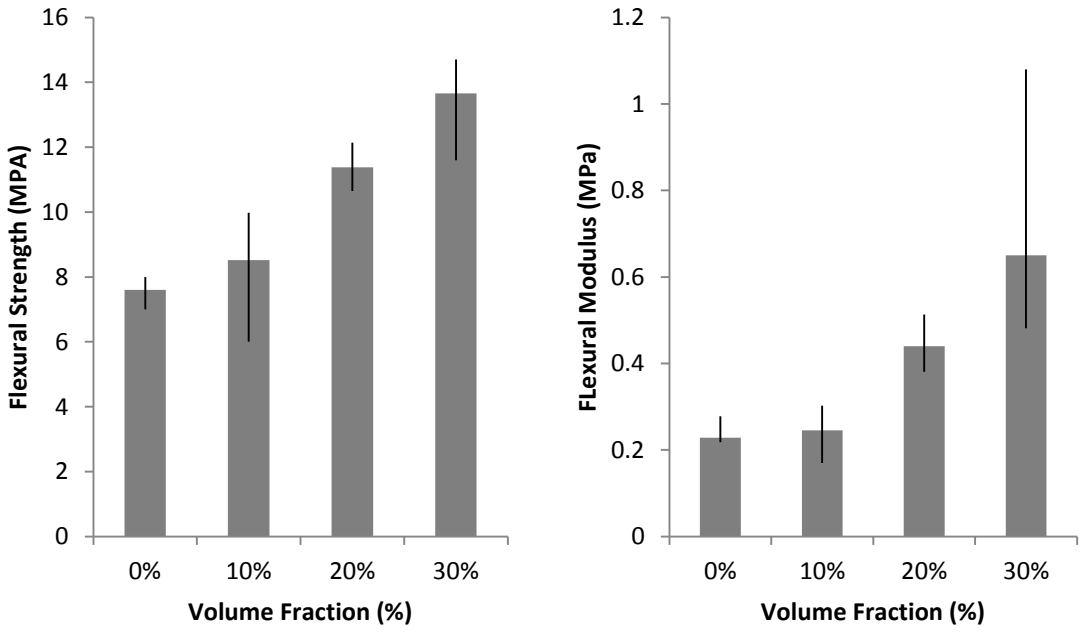

Figure 38 Flexural strength and modulus of 10%, 20% and 30% MAHEMP

Table 10 shows the flexural strength and modulus of 30% vol. fraction of MAHEMP composite. Figure 38 shows the bar chart for the above mentioned table. It

can be seen that the values for flexural strength and modulus increases consistently with the increase in fiber vol. fraction.

Figure 39. Shows the tensile tested specimen for 10% vol. MAHEMP

Figure 39 shows the tensile tested specimen of 10% vol. MAHEMP composites. The plasticizing effect of the polymer can be clearly seen in the picture due to high volume of the polymer in the composite.

Maleic anhydride grafted polyethylene is a chemical that has not been used in prior research to treat the fibers. Figure 37 shows the tensile strength and modulus of MAGHEMP composites. For 30% vol. MAGHEMP composite showed the superior results when compared with UNHEMP and NAHEMP. 30% vol. MAGHEMP specimen recorded 7.356MPa while NaOH and untreated composites showed 6.54MPa and 6.00MPa, respectively. The tensile modulus of 30% MAGHEMP composite also

showed the better result in comparison with UNHEMP and NAHEMP composites as well.

Figure 38 shows the flexural strength and flexural modulus of MAGHEMP composites. The flexural properties have improved significantly for the HEMP-LLDPE composite when treated with MA-g-PE. 30 vol% of Hemp composites showed the highest improvement in flexural strength and flexural modulus by 28.5% and 59.5%, respectively. Hence MA-g-PE treated composites showed superior results when compared with untreated and alkaline-treated composites for the tensile properties and flexural properties. One of the specimens of 30% vol. fraction showed 1.081 GPa whereas the rest had a half the values.

Figure 40 Failure of 10%, 20% and 30% vol. MAHEMP

Figure 40 shows the failures of 10%, 20% and 30% vol. of MAHEMP composite. The left specimen in 10% vol., while the middle and right is 20% and 30% vol. The difference can be seen and compared that lower fiber vol. have higher plastic effect to the composite. Due to higher fiber vol. the failure is classified as Lateral Gage Middle (LGM) according to ASTM for 20% and 30% vol.

Table 11 manifests the comparison of 30% vol. of HEMP-LLDPE for tensile strength, tensile modulus, flexural strength and flexural modulus. The values of the properties clearly show that Ma-g-PE improves the property of the composite. Therefore, it is concluded that MA-g-PE can be successfully used for the surface treatment of fibers. They are able to replace the hydroxyl group of the cell-wall and increase the fiber adhesion with the polymeric matrix.

Table 11 Comparison of 30% vol. of hemp in the composite

30 vol.% of hemp	Untreated	NaOH	MA-g-PE
Tensile strength (MPa)	6.0020	6.5400	7.3560
Elastic modulus (GPa)	0.5302	0.6702	0.6754
Flexural strength (MPa)	10.6320	11.9840	13.6600
Flexural modulus (GPa)	0.4128	0.5612	0.65842

5.2. Dispersive Nature of the Composite

NFCs are light weight and low density material. Compared to carbon fibers and glass fiber composites, NFCs are less stiff and highly dispersive in nature. Figure 41 shows the waveforms that were acquired in all the 8 directions of the specimen at loc. 1 and 3. The comparison in Figure 41 depicts the dispersive nature of the waves

propagating in the composite. The blue and red color represents the waveforms acquired from loc. 1 and 3 respectively, where Locations 1 and 3 are 1" and 3" far from the impact location along the same line. Figure 41 clearly shows the dispersion of the waveforms in all directions. The waves almost decayed within 0.02s of the impact. In time domain the amplitude represents energy. Therefore it is seen that the energy is dissipated. The polymer is known for its dispersive nature, but the addition of natural fibers adds to the dispersion, due to the low density and low stiffness of the natural fibers. Since lamb waves are sensitive to interference, randomly oriented fibers also avails in the dispersion of the waves. It can be concluded that if the fibers are unidirectional, then the waves propagating in the direction of fibers would be less dispersive and attenuative, while the wave propagating in perpendicular to the fiber alignment would have higher attenuation. Figure 42 shows the dispersion curve of the specimen in all 8 directions. A range of finite frequencies have been selected to shows the dispersion curve. Since it has been established that the waves are dispersive, and it is implied that as the frequency increases the (group) velocity of the propagating wave decreases. It can be seen that dispersion curves in Figure 42 follows a similar pattern where, as the frequency component increases the wave (group) velocity decreases.

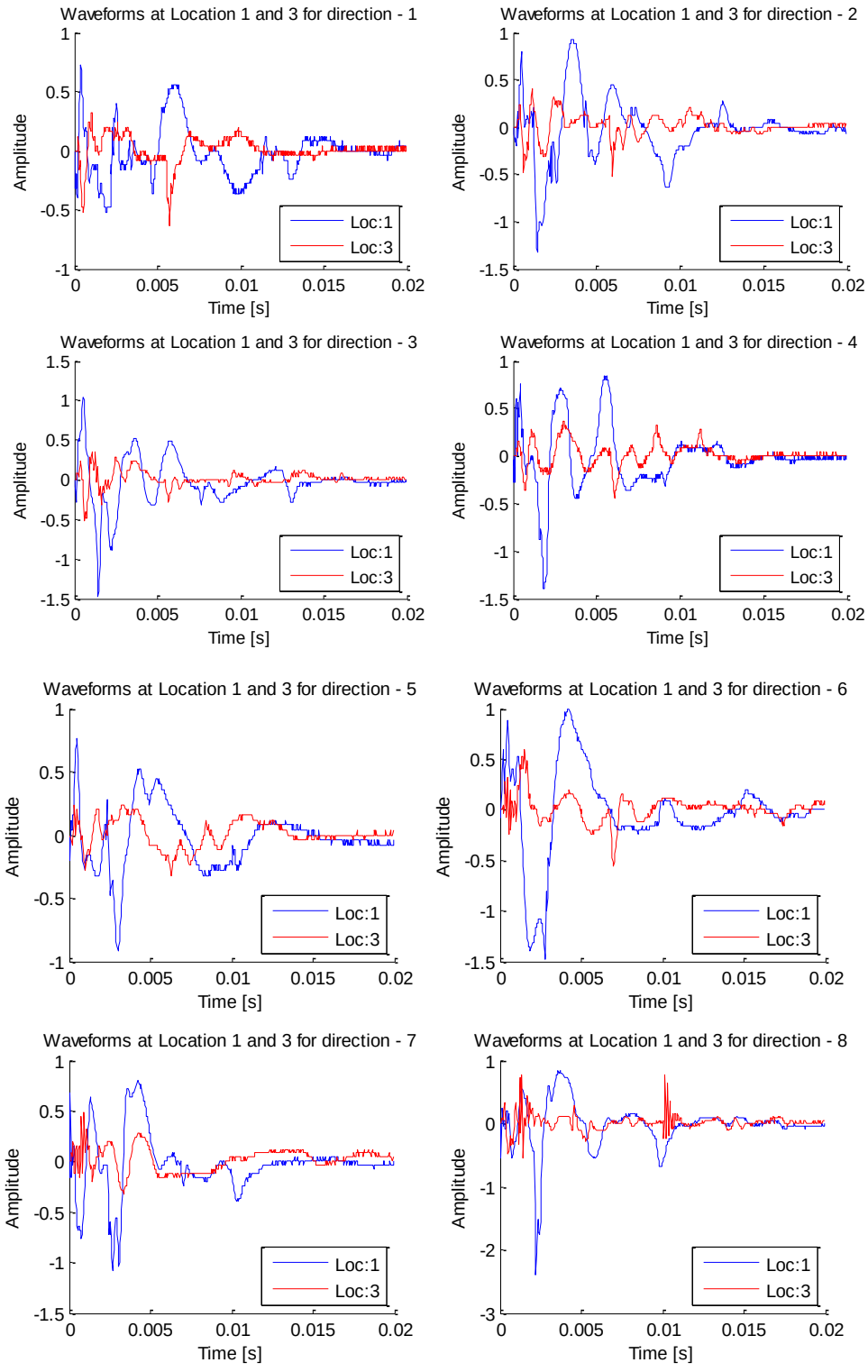

Figure 41. Waves acquired at location 1 and location 3 for all 8 directions

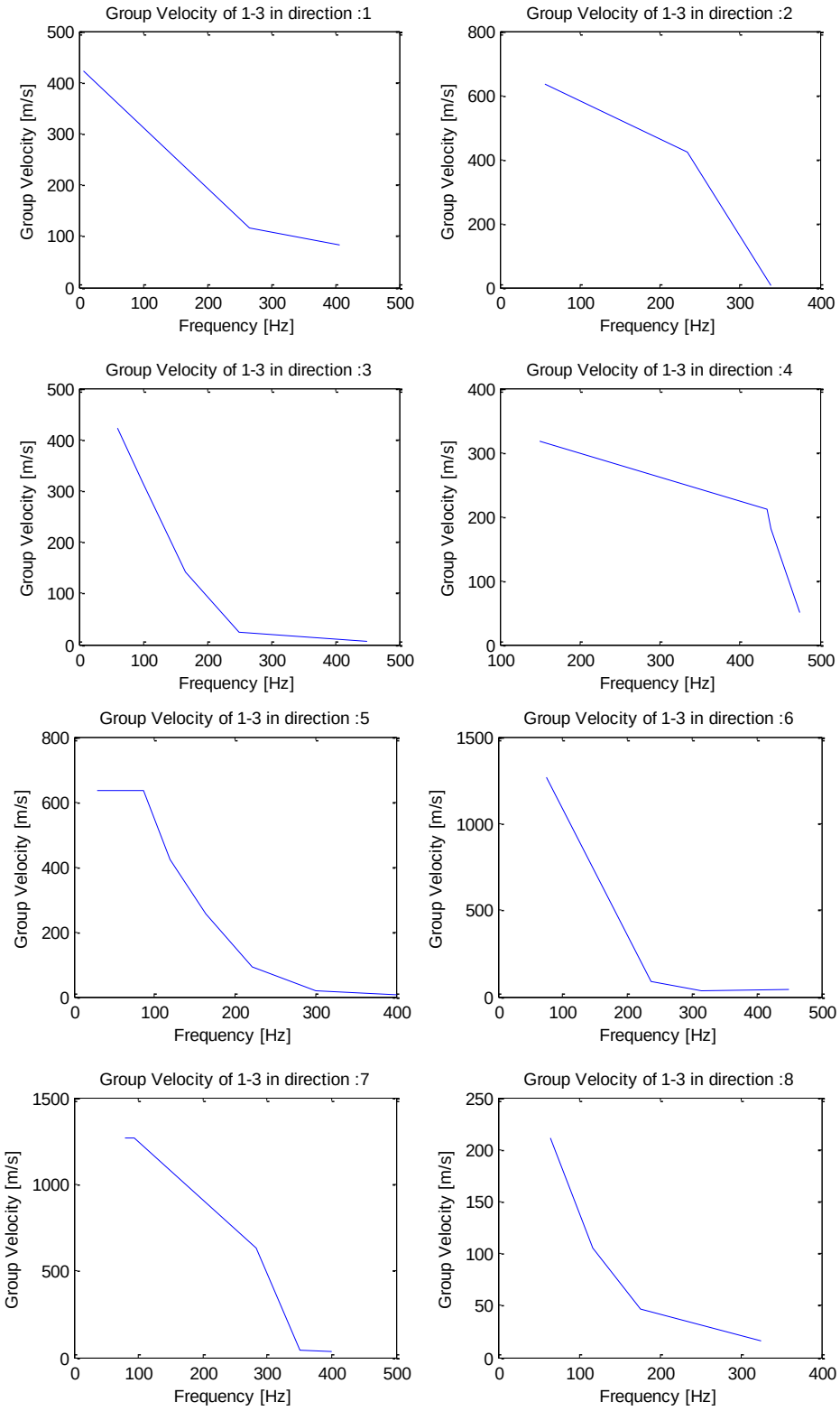

Figure 42. Dispersion curves in 8 directions

5.3. Homogeneity and Isotropy of the Composite

Figure 43 - Figure 50 show the GWT of the waves acquired in all the 8 directions. The images on the left are the GWTs of the waveforms acquired at Location 1 and the images on the right are the GWTs of the waveforms at Location 3.

On comparing the GWT images in Figure 43 - Figure 50 with the waveforms shown in Figure 41, it can be inferred that the material responses in the eight directions are not the same. In Figure 44, Figure 46 and Figure 49 for Location 1, the images look similar thus indicating the material properties may be similar in those directions but the rest of the images do not show any similarity which indicates that the properties are not similar in the rest of the directions. There are few possible reasons for it – randomly dispersed fiber with various lengths of fibers. The specimen went through two fabrication processes – melt mixing and compression molding, hence melt mixing plays a crucial role in proper fiber distribution. The fiber distribution varies during the fabrication of melt mixing. At the same time it should also be noted that the increase of fabrication process degrades the material property. The GWT images for Location 3 also show reflections from the edges of the circular specimen and the vibration of the specimen. The vibration of the specimen is depicted at 0.006s in the GWT images for Location 3, while the reflections of the waves are shown at different time instances in the GWT images. The reflection from the edge of the specimen creates a constructive interference which is also being shown in a few of the images. Figure 50 is an example of such a reflection for Location 3.

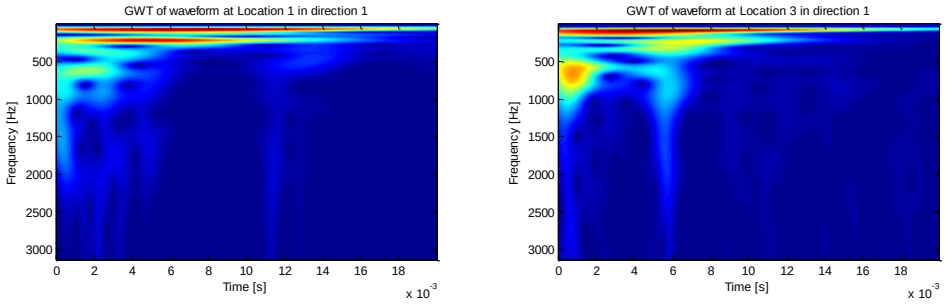

Figure 43. GWT of the waveforms in direction 1 for location 1 on the right and location 3 on the left.

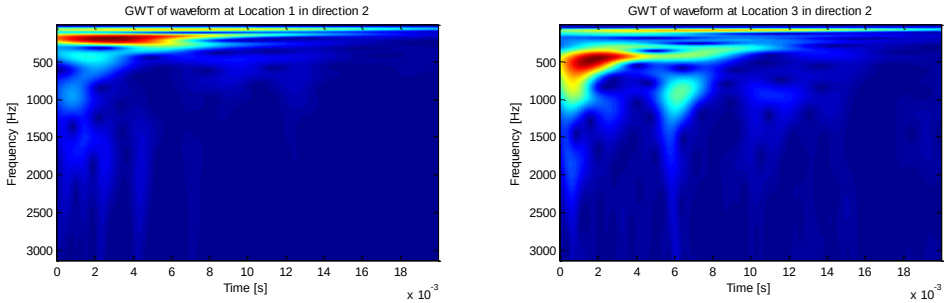

Figure 44. GWT of the waveforms in direction 2 for location 1 on the right and location 3 on the left.

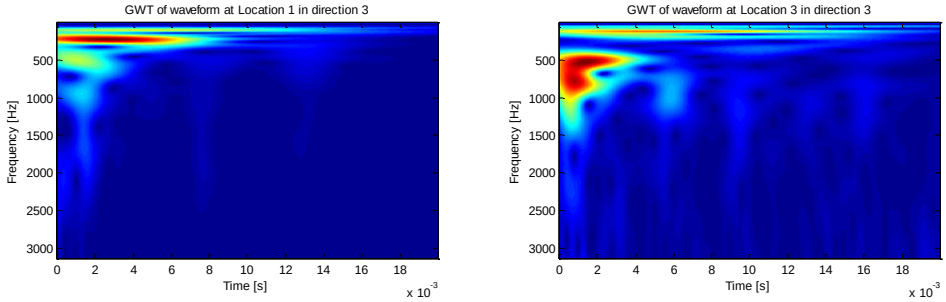

Figure 45. GWT of the waveforms in direction 3 for location 1 on the right and location 3 on the left.

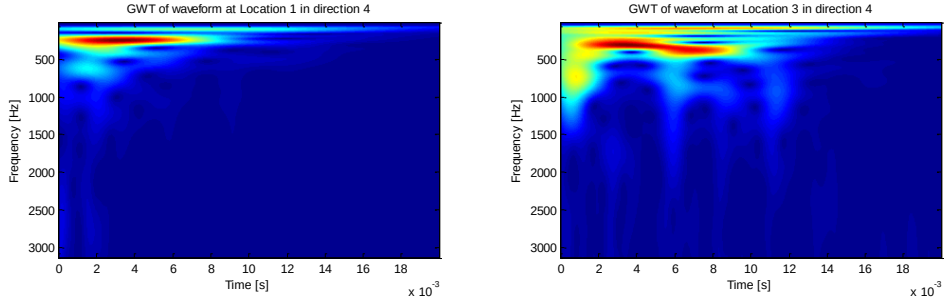

Figure 46. GWT of the waveforms in direction 4 for location 1 on the right and location 3 on the left.

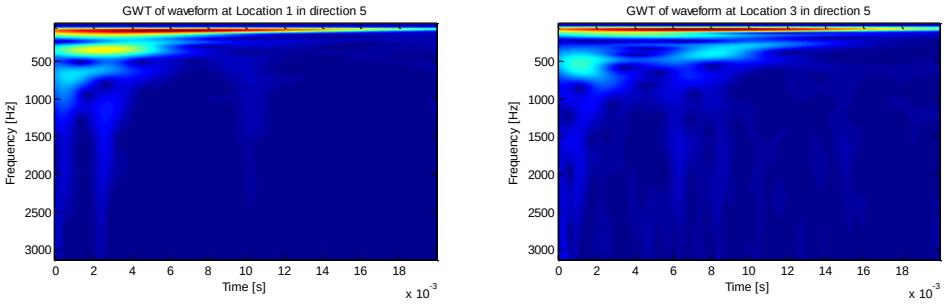

Figure 47. GWT of the waveforms in direction 5 for location 1 on the right and location 3 on the left

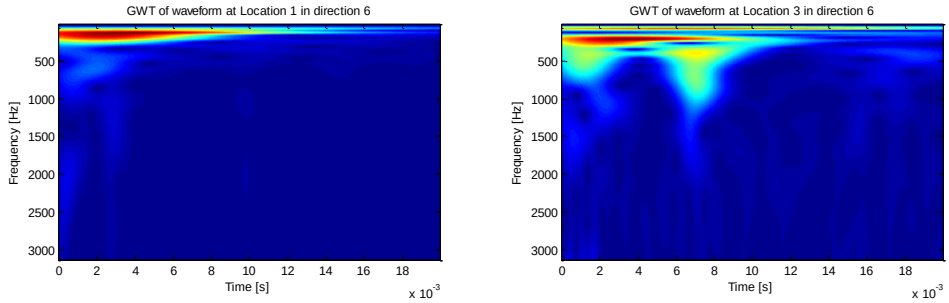

Figure 48. GWT of the waveforms in direction 6 for location 1 on the right and location 3 on the left.

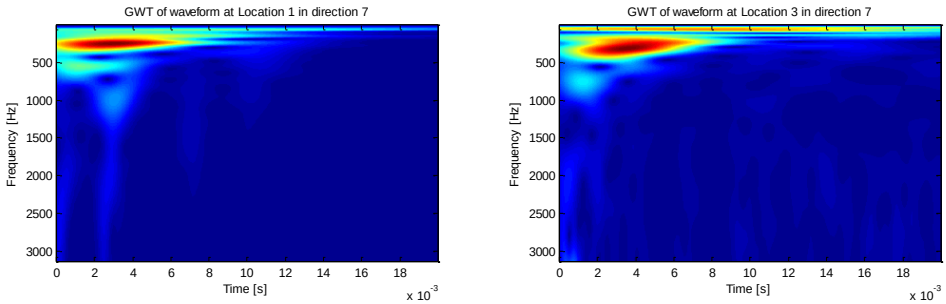

Figure 49. GWT of the waveforms in direction 7 for location 1 on the right and location 3 on the left

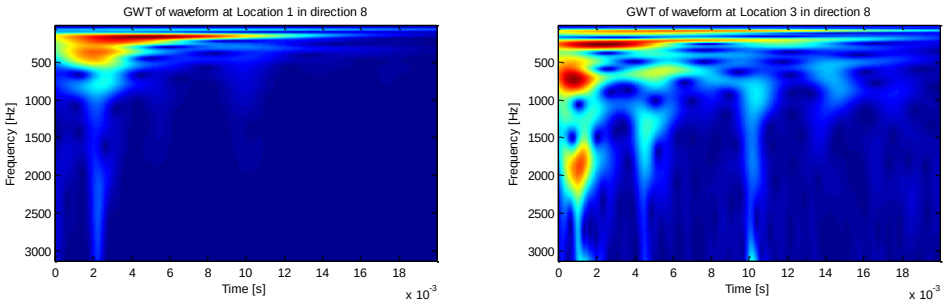

Figure 50. GWT of the waveforms in direction 8 for location 1 on the right and location 3 on the left.

5.4. Attenuation and Impact Resistance

The natural fiber composite shows a significant attenuation. Figure 51 - Figure 54 present the attenuation factor plotted against frequency in four directions.

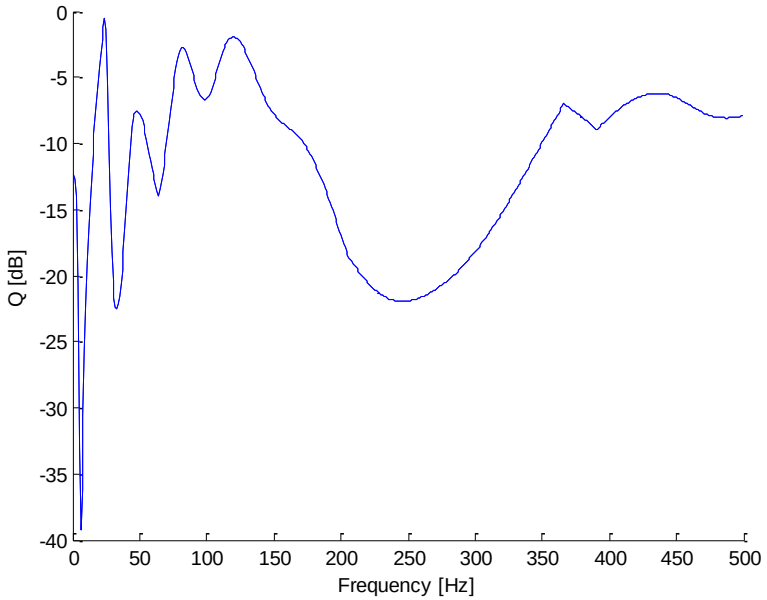

Figure 51. Attenuation in direction 1 between location 1 and 3.

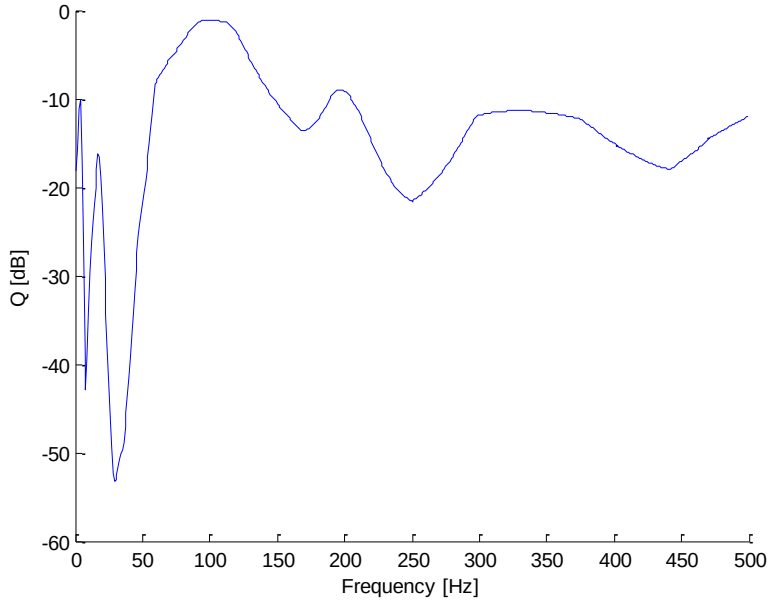

Figure 52. Attenuation in direction 2 between location 1 and 3.

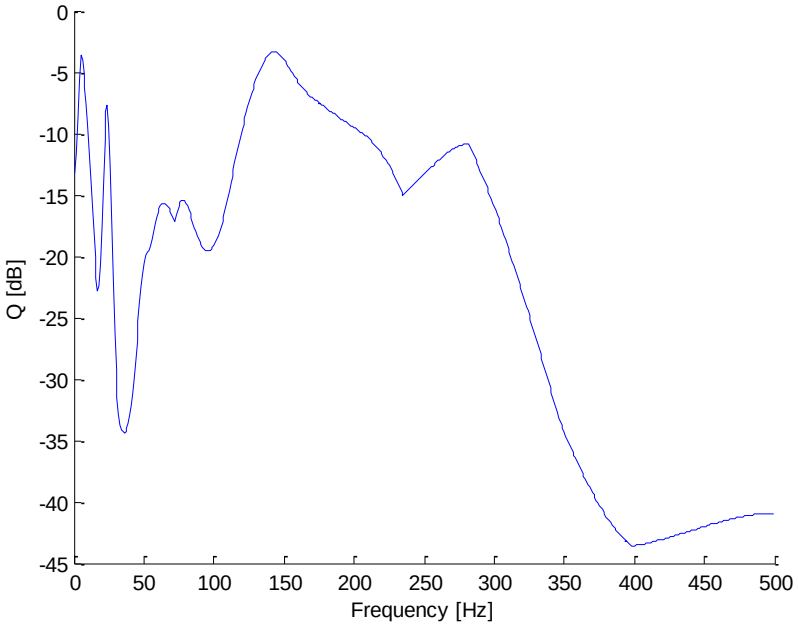

Figure 53. Attenuation in direction 4 between location 1 and 3.

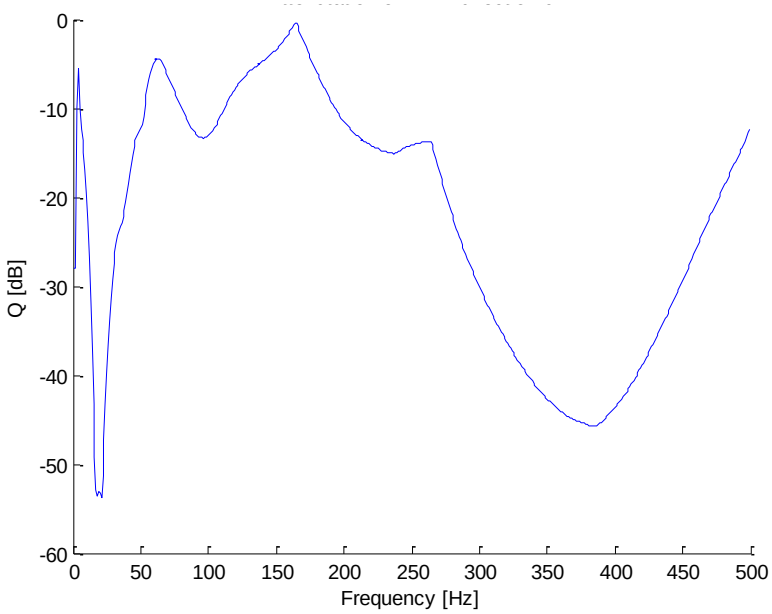

Figure 54. Attenuation in direction 6 between location 1 and 3.

It can be inferred from the above figures that the specimen has high attenuation factor, Q, along the directions considered. If looked closely, attenuations are high for

wave frequencies less than 50Hz. Shown in Figure 54 the attenuation factor is as low as 53.7dB for direction 6. The attenuation factors of higher frequency components fluctuate and do not follow the same pattern when compared in Figure 51 - Figure 54. Direction 4 in Figure 53 shows signification attenuation as the frequency increases from 150Hz onwards, whereas for direction 2 in Figure 52, the attention is low when compared with direction 4 or direction 6. This also signifies that the attenuation factor is not consistent in all direction. The fluctuation of Q also suggests the non-linearity of the composite. Figure 53 and Figure 54 shows that for the 400Hz frequency the corresponding Q's drop to 43 and 44 dB, respectively.

Carlomfirescu and Hermann [35] employed Lamb waves to measure the attenuation of a CFRP composite. They predicated the attenuation using Fiberwave software as well as experimentally. Figure 55 shows the attenuation curve of the CFRP, which they measured with a unit of dB/mm. Using interpolation, the attenuation of the predicted curve (red line) can be measured as 0.01dB/mm for the 5kHz frequency component and experimentally (black dot) as 0.01dB/mm for the 50kHz frequency component. Since Q is dB per unit distance, it can be converted as 1.016dB for 5kHz and 50kHz Figure 56 shows the attenuation of the NFC in direction 2. It can be seen that for the 5kHz frequency component the corresponding Q is -8dB which is clearly higher than the corresponding Q obtained for the CFRP. Therefore it can be established that the NFC has higher attenuation than the CFRP.

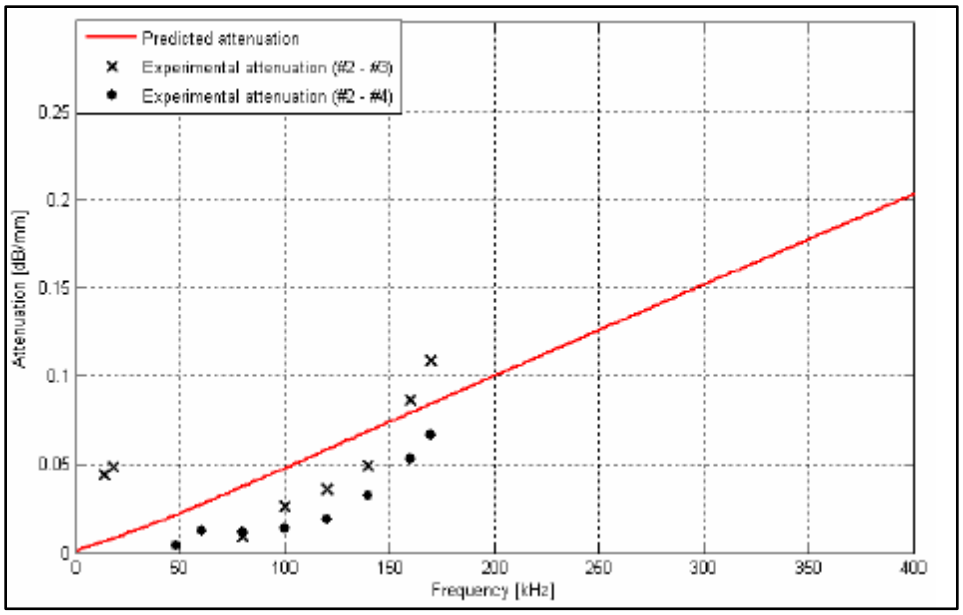

Figure 55. The attenuation of CFRP [35]

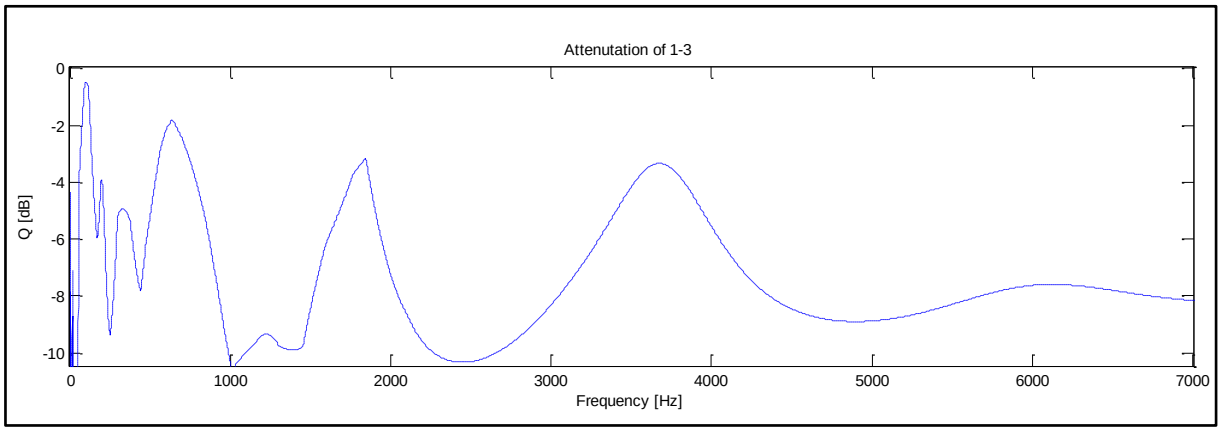

Figure 56. Attenuation of NFC in direction 2

5.5. Damage Detection

Three different types of damages were inflicted and pre-damage and post-damage waveforms were acquired at Location 3. The corresponding waveforms and attenuation factors are compared below.

Damage in direction 1: Figure 57 compares the waveforms and the Q acquired for Location 3. From the attenuation curve it can be learnt that for very low frequency wave the Q spikes down. It can also be inferred that the infliction of the dent shows higher attenuation for low-frequency wave when compared with the pre-damage waveform attenuation. The Q-factor corresponding to 50Hz and higher components reflects that a small dent in the specimen also attenuates the high frequency components. The attenuation curve looks similar for both waveforms, with an amplification of attenuation for the damage-inflicted waveform.

Damage in direction 2: The influence of the hole as a physical damage on attenuation Q works in similar fashion as the dent in the previous section. There are similar spikes for low frequency wave components, i.e. frequencies less than 50Hz. The hole also attenuates the frequency components higher than 50Hz as it can be seen in Figure 58.

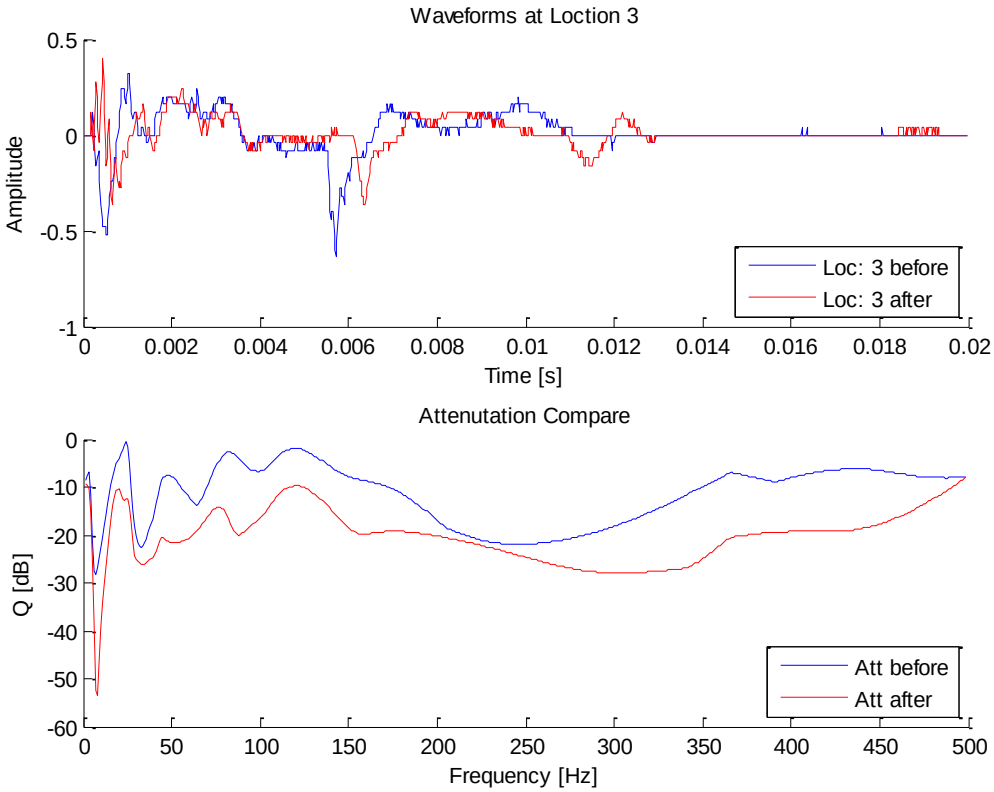

Figure 57. Comparison of waveforms and attenuation of location 3 in direction 1, blue color corresponds for pre-damage and red color corresponds for post damage.

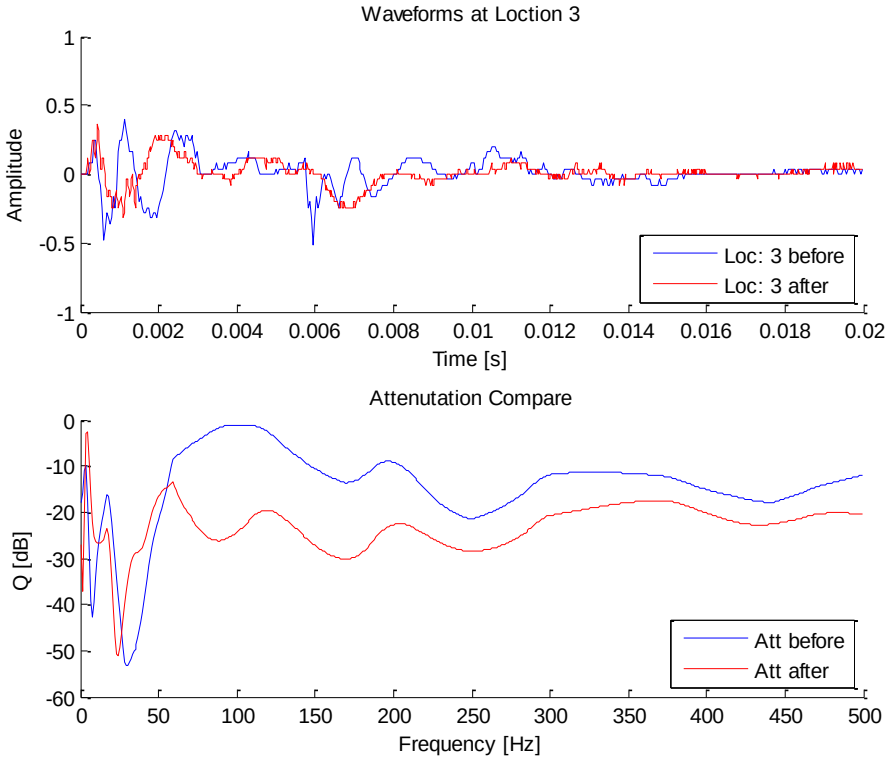

Figure 58. Comparison of waveforms and attenuation of location 3 in direction 2 with blue representing pre-damage and red color representing post-damage

Damage in direction 3: In direction 3, the damage was a shallow cut to depict a surface crack in the composite. The waveforms and attenuation curve are shown in Figure 59. The low frequency waves show very high attenuation while the high frequency waves show low attenuation. The pre-damage and the post-damage attenuation curves for high frequency waves are narrow and overlap at several instances. Figure 59 also shows that the two attenuation curves are very similar and close to each other, suggesting that narrow cuts and cracks do not attenuate waves like a hole or a dent does. It gives an impression that a shallow cut or crack is almost insensitive to the propagating waves.

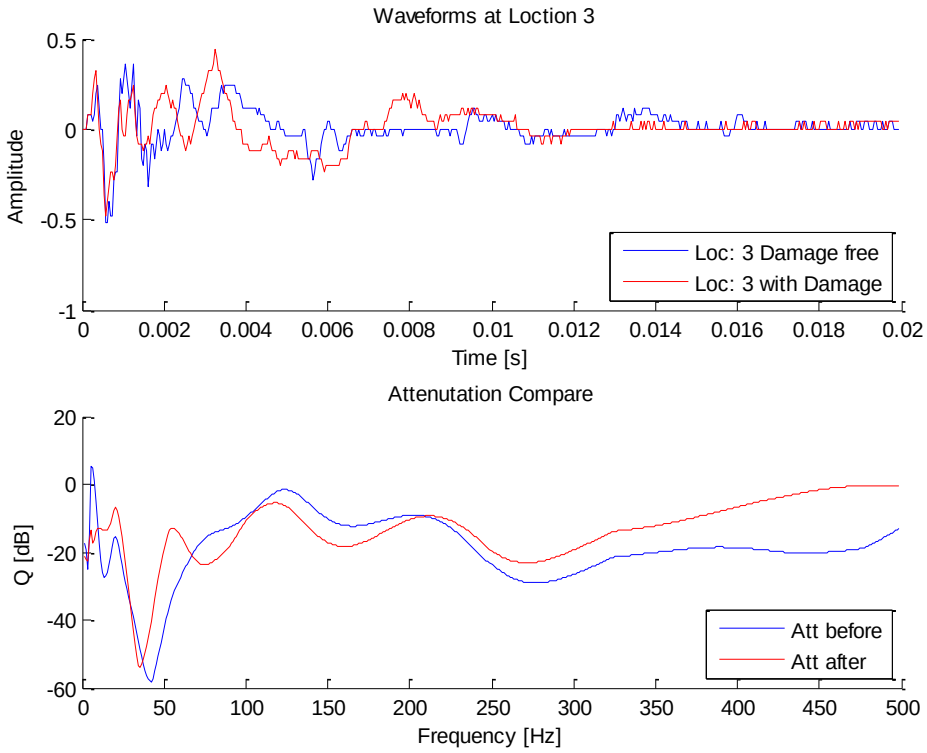

Figure 59. Comparison of waveforms and attenuation of location 3 in direction 3, blue color corresponds for pre-damage and red color corresponds for post damage.

6. CONCLUSION AND FUTURE WORK

6.1. Conclusion

The primary objective of this research was to study new composite HEMP – LLDPE and explore its static and dynamic properties. The aim was to use signal processing tools and feature extraction methodology to explore the characteristics of the material.

With the use of Lamb waves, this research was able to explore the homogeneity property of the thin disc specimen made from the composite. The GWT of the waves acquired showed that the properties of the composite were not the same in all directions. It was concluded that the fibers were not evenly distributed to provide homogeneity. There could be various reasons for non-uniform distribution of the fibers and having inhomogeneous property. A few of them are speculated below, as it was mentioned earlier, the chemical constituents of the fibers that influence the mechanical properties are dependent on the growing conditions. Hence each batch of the fibers grown may not have similar material strengths.

There is also a requirement of finding the optimal processing time. Since the natural fibers have a thermal degradation temperature of 230°C [2], therefore it is imperative to avoid overheating the fibers to prevent degradation. It is also required to find an optimal temperature where the viscosity of the polymer could avail the blending and proper dispersion of the fibers without degrading the strength of the fibers.

GWT is a great tool to employ for characterizing the materials. Using GWT, the attenuation factor was calculated for the specimen in different directions. The composite

showed a significant attenuation for very low frequency components and also for high frequency components. Carbon fiber composite, glass fibers composite and metals are comparatively stiffer, therefore the waves they support can propagate a longer distance with higher frequency and less attenuation. Waves in such materials can be highly destructive. If a material does not attenuate and disperse waves fast enough then the reflection of the waves from the edges can cause constructive interference and has the potential to cause serve damages to the material such as delamination in composites and cracks in metals, to name few. NFC is relatively compliant, hence capable of attenuating and dissipating waves within a short distance.

Damping factor plays a critical role in the dynamic properties of a material. Apart from the fibers and polymers, there are other factors that could also dampen waves. In this research there were three different types of damages inflicted: a hole, a dent and a series of superficial scratch to depict cracks. Using the GWT, the attenuation factor was obtained to characterize post-damage behavior of the material. It was shown that a propagating wave in the material is significantly attenuated when interfered by a dent or a hole. The cracks did not alter the propagation of low frequency waves, but it was seen that for higher frequencies or shorter wavelengths, the attenuation was less prominent. Therefore it was concluded that HEMP-LLDPE is considered viable to use with a small or shallow crack. Since a hole or a dent attenuates the wave, intentional defects can be created for design purposes to make a better sustaining material for dynamic loading. Applying artificial defects may avail in dynamic loading but such defects could potentially create catastrophic failure subject to static overloading.

Therefore to exploit such defects, it is critical to be aware of all kinds of loading involved.

This research also employed a chemical to provide a surface treatment on the fibers for better adhesion with the matrix. MA-g-PE has successfully provided a better adhesion and showed superior results than untreated and NaOH treated fiber composites.

Joshi et al [3] compares the density and price of glass fibers and flax fibers that are used in composites. They mentioned the price of glass fibers to be between $1.30 and $2.00/kg with a density of ~2.6g/cm^3 and the flax fibers cost between $0.22 and $1.10/kg with a density of ~1.5g/cm^3. Hence natural fibers are almost half the density and half the price of glass fibers. It was also mentioned earlier that NFCs require low energy consumption for fabrication than GFRP composites, thus implying low production cost for NFCs as well. Hence it is evident that NFCs are cost effective.

6.2. Future Work

Wave propagation can be applied to address a wide set of needs associated with the quality, manufacturing, and characterization of natural fiber composites including but not limiting to the followings:

- Usage of Lamb waves to inspect NFCs – Lamb waves are known to be sensitive to interferences. Hence further investigation can be done in NFCs to inspect for flaw and defect including delamination, cavity, and inhomogeneity, to name a few. Lamb waves can also be employed to characterize the types of defects.

- Usage of long natural fibers for better dynamic properties – long fibers extracted from plant can be reinforced into polymers without grinding into small sizes. It can be speculated that due to the long fibers it may use substantial amounts of energy to blend the fibers. But due to the larger dimensions of the fibers in the polymers, higher attenuation factor – Q may be achieved.
- Using fillers in NFC – Since it has been established that the mechanical properties of NFC not at par with CFRP and GFRP, injection of metal fillers or ceramic fillers can improve the static mechanical properties of the composites.
- Moisture absorbed NFC – Moisture absorbed specimens may have been proved of having inferior static mechanical properties, but such specimens may have the ability to dampen stress waves. Hence more testing could be performed to characterize moisture absorbed NFCs for dispersion and attenuation so as to establish their dynamic performance.

REFERENCES

[1] Chung DDL. Composite materials : science and applications. 2nd ed. London, UK: Springer; 2010.

[2] Saira T, Munawar MA, Khan S. Natural fiber-reinforced polymer composites. Pakistan Academy of Sciences. 2007; 44(2): 129-144.

[3] Joshi SV, Drzalb LT, Mohanty AK, Arorac S. Are natural fiber composites environmentally superior to glass fiber reinforced composites?. Composites Part A: Applied Science and Manufacturing. 2004; 35(3): 371-376.

[4] Li X, Tabil LG, Panigrahi S. Chemical treatments of natural fiber for use in natural fiber-reinforced composites: A Review. Journal of Polymers and the Environment. 2007; 15(1): 25-33.

[5] Pickering KL. Properties and Performance of Natural-Fibre Composites in Materials. Cambridge, UK: Woodhead Publishing; 2008.

[6] Leaf fibre. Encyclopædia Britannica Online. 2012; Available from: http://www.britannica.com/EBchecked/topic/333793/leaf-fibre. July 2012.

[7] McCrady E. The Nature of Lignin. Alkaline Paper Advocate 1991; Available from: http://cool.conservation-us.org/byorg/abbey/ap/ap04/ap04-4/ap04-402.html. July 2012.

[8] Jayaraman J. The effect of heat treatment on the structure and properties of sodsoi/PLA composites. MS Thesis. Hamilton, New Zealand: The University of Waikato; 2010.

[9] Ray D, Sarkar BK, Rana AK, Bose NR. Effect of alkali treated jute fibres on composite properties. Bulletin of Materials Science. 2001; 24(2): 129-135.

[10] Morrison Iiia WH, Archibald DD, Sharma HSS, Akin DE. Chemical and physical characterization of water- and dew-retted flax fibers. Industrial Crops and Products, 2000; 12(1): 39-46.

[11] Rong MZ, Zhang MQ, Liu Y, Yang GC, Zeng HM. The effect of fiber treatment on the mechanical properties of unidirectional sisal-reinforced epoxy composites. Composites Science and Technology. 2001; 61(10): 1437-1447.

[12] Agrawal R, Saxena NS, Sharma KB, Thomas S, Sreekala MS. Activation energy and crystallization kinetics of untreated and treated oil palm fibre reinforced phenol formaldehyde composites. Materials Science and Engineering: A. 2000; 277(1–2): 77-82.

[13] Sawpan MA, Pickering KL, Fernyhough A. Flexural properties of hemp fibre reinforced polylactide and unsaturated polyester composites. Composites Part A: Applied Science and Manufacturing. 2012; 43(3): 519-526.

[14] Chand N, Fahim M. Tribology of Natural Fiber Polymer Composites. London, UK: Woodhead Publishing; 2008.

[15] Mohanty S, Nayak SK, Verma SK, Tripathy SS. Effect of MAPP as a coupling agent on the performance of jute-PP composites. Journal of Reinforced Plastics and Composites. 2004; 23(6): 625.

[16] Kim H. Melt mixers in polymer processing lab. The Macosko Research Group. 2010; Available from:

http://research.cems.umn.edu/macosko/PDFS/MacoskoGroupMeltMixerOverview.pdf. July 2012.

[17] Chanda M, Roy SK. Plastic Technology Handbook. 4th Edition. Boca Raton, USA: CRC Press; 2007.

[18] Ruihua H, Lim JK. Fabrication and mechanical properties of completely biodegradable hemp fiber reinforced polylactic acid composites. Journal of Composite Materials., 2007; 41(13): 1655-1669.

[19] Beckermann G. Performance of hemp-fibre reinforced polypropylene composite materials. Materials and Process Engineering. PhD Thesis. Hamilton, New Zealand : The University of Waikota; 2007.

[20] Na L, Swan Jr RH, Ferguson I. Composition, structure, and mechanical properties of hemp fiber reinforced composite with recycled high-density polyethylene matrix. Journal of Composite Materials. 2012; 46(16): 1915-1924.

[21] Keller A. Compounding and mechanical properties of biodegradable hemp fibre composites. Composites Science and Technology. 2003; 63(9): 1307-1316.

[22] Dhakal HN, Zhang ZY, Richardson MOW. Effect of water absorption on the mechanical properties of hemp fibre reinforced unsaturated polyester composites. Composites Science and Technology. 2007; 67(7–8): 1674-1683.

[23] Hu R, Lim JK. Fabrication and mechanical properties of completely biodegradable hemp fiber reinforced polylactic acid composites. Journal of Composite Materials. 2007; 41(13): 1655-1669.

[24] Kabamba ET, Mechraoui A, Rodrigue D. Rheological properties of polypropylene/hemp fiber composites. Polymer Composites. 2009; 30(10): 1401-1407.

[25] Bledzki AK, Fink HP, Specht K. Unidirectional hemp and flax EP- and PP-composites: Influence of defined fiber treatments. Journal of Applied Polymer Science. 2004; 93(5): 2150-2156.

[26] Worlton DC. Experimental confirmation of Lamb waves at megacycle frequencies. Journal of Applied Physics. 1961; 32(6): 967–971.

[27] Su Z, Ye L, Lu Y. Guided Lamb waves for identification of damage in composite structures: A review. Journal of Sound and Vibration. 2006; 295(3–5): 753-780.

[28] Worden K, Manson G, Allman D. Experimental validation of a structural health monitoring methodology: Part I. Novelty detection on a laboratory structure. Journal of Sound and Vibration 2003; 259 (2): 323–343.

[29] Graff KF. Wave Motion in Elastic solids. Mineola, USA: Dover Publication; 1991.

[30] Liu L. Elasto-Viscoplastic wave propagation in a single crystallographic silicon thin structure. MS Thesis. College Station, USA: Texas A&M University; 2005.

[31] Harms KD, Suh CS. Laser-Optic evaluation for bond quality of polymeric medical tubing. Journal of Pressure Vessel Technology. 2002; 124(3): 283-292.

[32] Shen L. Recognizing Faces --- An Approach Based on Gabor Wavelets. PhD Thesis. Nottingham, U.K: University of Nottingham; 2005.

[33] Schubert KJ, Herrmann AS. On attenuation and measurement of Lamb waves in viscoelastic composites. Composite Structures. 2011; 94(1): 177-185.

[34] Vedantham V. In-Situ temperature and thickness characterization for silicon wafers undergoing thermal annealing. MS Thesis. College Station, USA: Texas A&M University; 2003.

[35] Calomfirescu M, Herrmann AS. Theoretical and experimental studies of Lamb wave propagation in attenuative composites. In: Proc. SPIE 6529. Sensors and Smart Structures Technologies for Civil, Mechanical, and Aerospace Systems. 2007; 652929.